الجمـــهوريـــة الجـــزائريـــة الديـمقراطيـــــــة الشـــعبيـــــة
THE PEOPLE'S DEMOCRATIC REPUBLIC OF ALGERIA
وزارة التعـلـيـم الـعـالـــي والـبـحـث الـعـلـمي
THE MINISTRY OF HIGHER EDUCATION AND SCIENTIFIC RESEARCH
جـامـعـة عمّـــار ثـلـيـــجـــي بالأغـــواط
AMAR TELIDJI UNIVERSITY OF LAGHOUAT

كـلـيـــــة الـتكنولوجيا
FACULTY OF TECHNOLOGY

قسم الالكتروتقني
DEPARTMENT OF ELECTROTECHNIC

Master's thesis

Domain :	Sciences and Technologies
Field :	Automatic
Option :	Automatic and systems

Theme

Control of Parallel Inverters in a Microgrid

Presented by:
Mr. Aissa SEGHIER
Mr. Ali BEDJ

Publicly supported ahead of a jury composed of :

Mr. Bachir BENDJEDIA	*M.C.A*	*President*
Mr. Mohammed BENMILOUD	*M.C.B*	*Examiner*
Mr. Atallah BENALIA	*Prof.*	*Supervisor*
Mr. Mohammed Djameleddin BOUGRINE	*M.C.B*	*Co-supervisor*
Mr. Mohammed ELamine BENZOUBIR	*PhD student*	*Guest*

Academic year 2021/2022

Acknowledgments

With the help of Almighty God, we were able to accomplish this work, which was carried out within the LACoSERE laboratory and the electrical engineering department at Amar Telidji University of Laghouat.

At the end of this work, we would like to thank our supervisor Mr. Atallah BENALIA for his support, guidance and constructive criticism.

We would like to thank our co-supervisor Mr. Mohammed Djameleddine BOUGRINE for his enormous follow-up, for his constant attention to our work, for his wise advice and his listening, which were essential for the success of this dissertation, and for his confidence.

We would like to thank Mr. Mohammed ELamine BENZOUBIR (PhD student) who helped us a lot.

We also thank all of those who contributed from near or far to the realization of this work, who will find here our expression of our full gratitude and appreciation.

We would also like to thank the members of the jury for accepting to examine our work. Thank you for the constructive remarks, and for your relevant comments.

We would like to express our sincere thanks to the teachers who have guided us throughout this academic journey.

Dedication

First, I would like to thank **Allah** Almighty for giving me patience and strength to finish this work.
I dedicate this modest work :

To my dear and beloved mother and father who have paved the path that i walked on and done everything for me to succeed in my life and wished nothing but the best for me, may Allah protect them.

To my soft-hearted brothers ABDELMADJID and SALAH as well as my admirable sister HABIBA who have shown me support and filled me with encouragements during these years of study.

To my partner Ali for his serious work.

To my friends R.WAIL, B.SALAH, G.HARZALLAH and B.ABDELMADJID for their friendship, unconditional support and encouragement.

Aissa SEGHIER.

Dedication

First of all, this work would not be possible without the help of all mighty god, and He who does not thank people, does not thank **Allah**. This work is dedicated to :

A loving mother and grandmother, Dr. Maicha Yamina and Menaa Atika, who were there giving me strength and unconditional support from day one, through thick and thin, i wouldn't be half of the man that i am today without them , and for that, i thank them.

My grandfather, Maicha Lalmi, who even in sickness, expresses concern and curiosity in my work, as well as his brother, my uncle, Maicha Ahmed, who never ceased from encouraging me through all of the hardships.

A caring father and a thoughtful uncle as well as a perfect aunt in law, Bedj Rachid, Bedj Fadel and his wife, who despite whatever rock might get in the way, give an example and inspiration to the stubborn kid that's in me, Thank you.

A relentless partner with an inspiring work ethic, Seghier Aissa.

Every student, classmate and teacher that i have had the honour of working with or learning under, Thank you.

Ali BEDJ.

Abstract

A worldwide shift towards more sustainable types of energies is being led by researchers worldwide, and the introduction of microgrids to integrate those types of energies is becoming more needful. This dissertation interests to the control of parallel inverters. The control is hierarchical in the sense that it should be carried out upon several levels, starting from the controlling of each inverter in voltage or current, then ensuring the power sharing between them using techniques like Master/Slave control and Droop control and finally implementing a voltage amplitude and frequency restoration for the Droop control method.

Keywords: Microgrids, Parallel inverters, Sliding mode control, Power sharing, Droop Control, Master/Slave control.

ملخص

يقود الباحثون في جميع أنحاء العالم تحولًا عالميًا نحو طرق إنتاج للطاقة أكثر إستدامة ، كما أن إدخال الشبكات الصغيرة لدمج هذه الأنواع من الطاقة أصبح ذا أهمية متزايدة. تتناول هذه المذكرة التحكم في المموجات الكهربائية المتصلة على التوازي . يكون التحكم بشكل هرمي بمعنى أنه يحدث على عدة مستويات ، بدءًا من التحكم في كل مموج في الجهد أو التيار ، ثم ضمان تقاسم الطاقة بينهما باستخدام تقنيات مثل تقنية المتحكم/التابع وتقنية التدلي وأخيراً من خلال تنفيذ استعادة التوتر الأعظمي والتردد لتقنية التدلي.

كلمات مفتاحية : شبكات صغيرة (ميكرو شبكات) , مموجات كهربائية على التوازي , التحكم بوضع الإنزلاق , مشاركة الطاقة , وضع التدلي , تقنية المتحكم/التابع.

Résumé

Une évolution mondiale vers des types d'énergies plus durables est menée par des chercheurs du monde entier, et l'introduction de micro-réseaux pour intégrer ces types d'énergies devient de plus en plus une exigence. Ce mémoire s'intéresse à la commande des onduleurs parallèles. La commande est hiérarchique dans le sens où elle doit se faire sur plusieurs niveaux, commençant par le contrôle de chaque onduleur en tension ou en courant, puis en assurant le partage de puissance entre eux en utilisant des techniques comme la technique Maître/esclave et la technique de statisme et enfin en mettant en œuvre une restauration d'amplitude et de fréquence pour la technique de statisme.

Mots-clés : Micro-réseaux, Onduleurs parallèles, Commande par mode glissant, Partage de puissance, Technique de statisme, Technique Maître/Esclave.

Acronyms

AC: Alternative current

DC: Direct current

PID: Proportional–Integral–Derivative

MGs or µGs: Microgrids

DER: Distributed Energy Resources

DES: Distributed Energy Storage

DG: Distributed Generators

CHP: Combined Power and Heat

PCC: Point of Common Coupling

VSI: Voltage Source Inverter

CSI: Current Source Inverter

SMC: Sliding Mode Control

FOSMC: First Order Sliding Mode Control

HOSMC: Higher Order Sliding Mode Control

SOSMC: Second Order Sliding Mode Control

PWM: Pulse Width Modulation

emf: Electromotive force

.

Contents

List of Tables

List of Figures

General Introduction

World electricity production is experiencing sustained growth to meet the increase in electrical energy needs and support countries' development efforts. These efforts come up against increased greenhouse gas emissions due to global warming. These efforts are accompanied by measures to begin the energy transition to sustainable and green energy. For example, Algeria is embarking on a new sustainable energy era. The Renewable Energy Program in its updated version, consists of installing a renewable source power of the order of 22,000 MW by 2030 for the national market, with the maintenance of the export option as a strategic objective, if market conditions permit.[8]

As part of our work, we are interested in the study of autonomous AC micro-grids composed of two distributed generators. The objective is to control this micro-grid.

This thesis was made as part of the Master's curriculum in automatic and systems, at the LACoSERE lab. at the University of Laghouat. This work is divided into three chapters:

In chapter I, a bibliographical study on the context of the distributed generation of electricity and the various control techniques developed in the literature is presented. More precisely, a state of the art on the different control techniques used for the voltage and current regulation for power sharing between the different distributed generators is presented.

In chapter II, a modeling of an inverter with LCL filter is carried out to design a control law for the system. To well understand the tools used in the subsequent chapter, a presentation of the control laws principles is given, namely PID and sliding mode controls. Chapter III presents the application of second-order sliding mode control of (twisting algorithm[6]) on two distributed generators to control the filter capacitors' voltages for the first inverter, and the output current for the second one as part of the zero level control. For a primary control we presented two methods, the first one is a centralized method known as Master/Slave scheme with central controller, and the second is a decentralized method that uses the droop control technique. The secondary control for the second method is also highlighted. Simulation results using MATLAB for each method are also given and discussed.

Finally, a conclusion that summarizes the work and some perspectives end the manuscript.

Chapter I

State of The Art on Microgrids

I.1 Introduction

Due to current environmental issues, the movement towards greener and environmentally friendlier energies became the leading subject of many audiences around the world whether they are coming from a political or a scientific point of view. In fact, these last years witnessed a huge movement towards developing electrical systems based on power electronics applications, which are then powered by a sustained and renewable sources of energy such as solar, wind, etc.

In this first chapter, we will explore the fundamentals of microgrids in general, their advantages and disadvantages, and their modes of operation. We will also speak of DC-AC converters, more commonly known as inverters, their types, and their relationship with microgrids. Finally, we will explore the different control strategies that can be applied to a parallel form of inverters in a microgrid.

I.2 What is a microgrid

Microgrids (MGs or µGs) cannot be understood as a new concept since small-scale power grids have existed for a long time in distant regions, where interconnection with the main grid is not possible for technical or economic reasons. Currently, the concept and definition of microgrids are changing to provide customers with sustainable energy choices in terms of renewable energy integration, grid reliability, flexibility and economy. A microgrid is defined as an energy system incorporating intelligent management and consists of a variety of components, including : distributed energy resources (DER) (photovoltaic, small wind turbines, fuel cells, etc.) and distributed energy storage (DES) devices (Supercapacitors, Batteries, etc.) that can be used to absorb the power excess from the grid and dump current to cover the power deficit. In a nutshull, it operates as a controllable load to help improve the reliability of the microgrid. Generally they are located nearby and they may include customers ranging from a single house

to a group of heavy loads (hospital, school or campus, military base). The characteristics and dynamics of each microgrid component presents a major challenge in controlling and operating with the main grid.[9]
According to the US department of energy's official website, a microgrid is a local energy grid with control capabilities, in other words, it can be disconnected from a provided traditional grid and operate autonomously or what is called "islanded mode".[10]

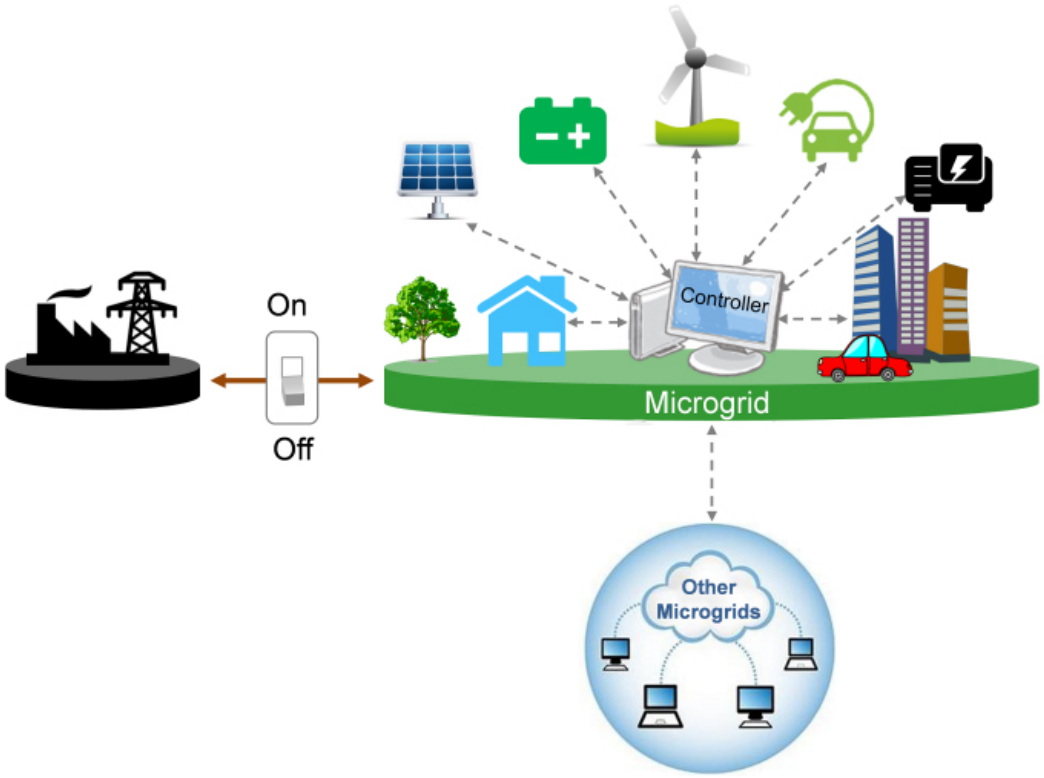

Figure I.1: Basic structure of a microgrid [2]

I.3 Advantages and disadvantages of MGs

Large energy users, from cities and colleges to industrial and military operations, have different needs. Some require a flexible power system to protect their communities in emergency situations, while others need to optimize their energy or protect their critical operations, and all of them aspire to greener energy sources. Whatever the reasons, customizable microgrid solutions provide optimal performance to meet a range of critical needs thanks to their different advantages:

Ensured reliability :

- System resilience: 24/7 service continuity with local energy generation. And provides a backup for the main grid in case of emergencies such as sudden power loss

- Power quality: assures good energy quality while maintaining stability and electrical safety.
- Power availability: assures enough power to respond to any given demand by balancing the supply of the main grid, local production, and load management and allows isolated geographic areas to be more energy independent

Optimal efficiency :

- Reduce losses: The proximity between production and consumption makes it possible to optimize the delivery of energy.
- Reuse heat: The use of both electricity and heat, which increases overall energy efficiency with the combined power and heat (CHP) system, which captures the resulting thermal energy from electricity production for a wide variety of thermal needs (hot water vapour, heating systems), which offers opportunities to optimize the DG.
- Cost: Limit investments in transport and distribution grids.
- Allows for isolated geographic areas to be more energy independent and in some cases more environmentally friendly.

Improve environmental sustainability :

- They make it possible to better integrate energies from renewable sources into the main grid and thus avoid the installation of thermal power plants.
- Store and exploit the energy so that it can be used when needed.
- Reduce greenhouse gas emissions and the carbon footprint.[11]

However, despite the advantages mentioned above, the MG has some drawbacks:

1. Voltage, frequency and power quality should be at acceptable limits, which poses a challenge when designing an adequate control law.
2. Requires battery tanks to store energy, which requires space and maintenance.
3. synchronization to utility grid is proven to be a difficult task
4. Microgrid protection is one of the most important challenges facing microgrid implementation.[9]

I.4 Types of microgrids

I.4.1 From a connection standpoint

Remote or islanded

These microgrids are disconnected from the utility or the traditional grids and they operate at all time in the island mode due to the lack of available and affordable transmission or distribution infrastructures nearby, utilized mainly as battery energy storage, their main energy sources are wind and sun.[12]

Grid connected microgrids

Opposed to the first type, these microgrids have the option of connecting to the grid using a switching mechanism at the Point of Common Coupling (PCC), they also have the option of working in island mode as well. In connected mode, they can provide grid services to the main or utility grid such as frequency and voltage regulation, real and reactive power support and power quality improvement.[12]

I.4.2 From an operational configuration standpoint

DC microgrids

DC microgrids connect the various energy generation sources and loads to a common DC bus. Typically, DC microgrids consist of distributed generation sources varying from renewable and conventional power generation sources such as engine-based generators. These are connected to each other through a DC bus. Renewable generators (solar photovoltaic panels, wind-turbines/rectifier system, batteries, etc.) produce DC output. The operational voltage of these DC buses often ranges from 350 to 400 Volts. [13]

AC microgrids

. The operational principle of AC microgrids is quite similar to their DC counterparts. The main difference between them is the usage of an AC bus network for interconnection rather than the DC bus which interconnects the distributed generators and loads in the network. this output can be converted into AC through power electronic-based converters (inverters) that need control systems, which is the main topic treated in this work.[13]

I.5 Definition of an inverter

DC-AC converters, also called inverters, are power electronic devices that makes it possible to transform a DC source into an AC source. This transformation is based on fast and robust control devices (semiconductor devices).[14] The symbolic representation of an inverter is shown in figure I.2:

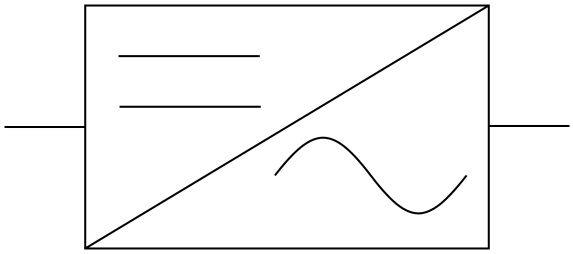

Figure I.2: Inverter's Symbol [3]

I.6 Classification of inverters

Inverters can be divided into two types according to their power source:

I.6.1 Voltage Source Inverter (VSI)

A VSI is an inverter fed by a DC-voltage supply, i.e. by a supply with negligible internal impedance; its voltage is not affected by the variations in current flowing through it. The DC supply imposes the voltage at the input - and thus at the output - of the inverter. If the voltage u is constant and equal to U, whatever the value of i,

$$\begin{aligned} &\text{for} \quad 0 < t < \frac{T}{2}; u' = +U \\ &\text{for} \quad \frac{T}{2} < t < T; u' = -U \end{aligned} \tag{I.1}$$

With T being the the operating cycle of the inverter and its output values. The output current i' and thus the input current i depend on the load placed on the AC side. This load can be of any type, provided that it is not another voltage source connected directly across the output terminals.[14]

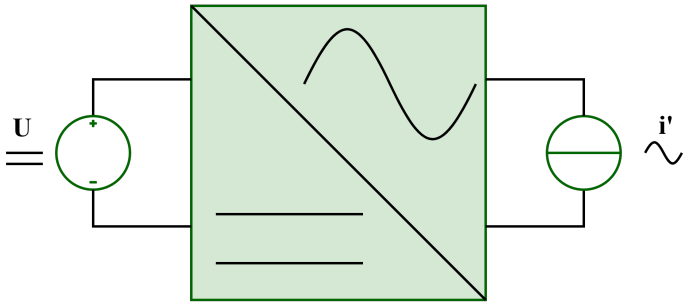

Figure I.3: Voltage source inverter [3]

I.6.2 Current source inverter (CSI)

A current-source inverter (also known as a current-commutator) is fed by a DC-current supply, i.e. by a supply whose internal inductance is too great that current i flowing through it cannot be affected by variations of voltage u across it - more especially by the discontinuities in u, corresponding to the commutations. The DC supply imposes the current waveform at the converter input and thus at its output. If i is constant and equal to I, whatever the value of u,

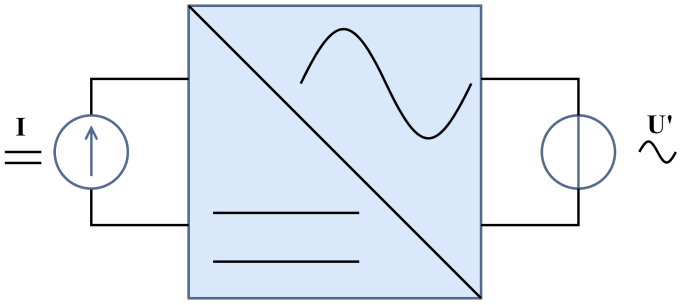

Figure I.4: Current source inverter [3]

$$\begin{aligned} \text{for} \quad & 0 < t < \frac{T}{2}; i' = +I \\ \text{for} \quad & \frac{T}{2} < t < T; i' = -I \end{aligned} \tag{I.2}$$

With T being the the operating cycle of the inverter and its output values. Voltage u' at the output and thus voltage u at the input are dependent on the load placed on the AC side. This load can be of any type, as long as it does not consist only of one current source.[14]
It can be also divided into two other types in regards to their control objectives, we have :

I.6.3 Grid following inverters

A grid following inverter is a DC-AC converter whose injected currents are controlled with a specific phase displacement in respects to the grid voltage at the point of common coupling. Having said that, the fundamental frequency of the grid at the PCC must be known at any

time for the correct calculation of the current's reference signal whose amplitude and angle with respect to the grid voltage phasor are properly modified by outer control loops which can then for example inject the right amount of active and reactive power.[13]

I.6.4 Grid forming inverters

Opposed to the grid following inverter, rather than controlling the currents, the magnitude and angle of the output voltage at the PCC is the control goal, with that been said, this type of inverter does not necessarily require the knowledge of the fundamental frequency at the point of common coupling.

A grid forming inverter has the ability to inject instantaneous active and reactive power and can provide voltage and frequency support.[13]

I.7 The purpose of using parallel inverters :

The primary concern of the usage of an inverter in a grid-connected situation can be summarized in providing reactive energy and maintaining a certain voltage and frequency in the cases of high-energy demand put on the traditional grid. With such a high power being delivered through an inverter, having a single one may have some issues including :

- Poor reliability: in the case of the inverter shutting down due to some fault, the whole microgrid will stop working.

- Maintenance and flexibility issues: having just one inverter can mean that its maintainability will lead to its shutdown and by extension the cease of the entire process connected to its output.

For these reasons, a parallel structure of inverters is one of the effective solutions to overcome the aforementioned issues, not only by helping to achieve a higher power rating, but also by improving the system's reliability as well. A parallel implantation of inverters is used to :

- Getting a reliable set of inverters when it comes to one of them being shut down or more due to different reasons such as components wear, accidents, etc.

- Keeping the system maintenance planning complexity at a low level, where in the case of one inverter, the whole system collapses but in the case of multiple parallel inverters, it would be a simple task.

I.8 Microgrid Control Strategies

Microgrids often benefit from an advanced control strategy intended to improve their performance. These strategies are mainly based on a hierarchical structure made up of four levels of control: level-zero, primary, secondary and tertiary as shown in figure I.5 :

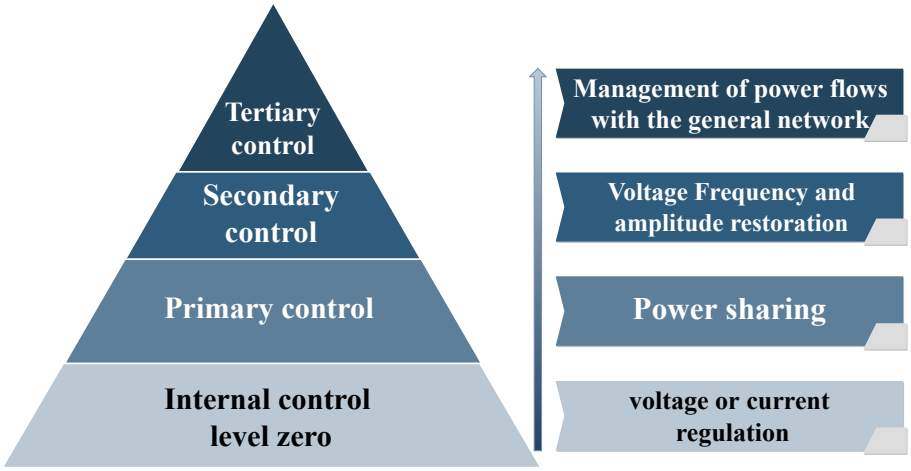

Figure I.5: Hierarchical control strategy [2]

I.8.1 Internal control (Level-zero)

This level of control is used to ensure the regulation of the voltage or the current at the output of each distributed generator (DG). It uses local measurements and does not require communication between the different DGs. The objective of this control is to ensure the tracking of the reference voltage/current wave robustly with respect to the installed loads [2]. The output voltage or current must be controlled in order to minimize its harmonic content in the presence of non-linear loads and to reduce the imbalance introduced by eventual unbalanced loads or the impact caused by the accidental disconnection of one of the phases.

I.8.2 Primary control

This hierarchical level of control is dedicated to the management of load distribution and active and reactive power flows between the various interconnected distributed generation units. This control makes it possible to determine the reference voltage to apply to each distributed generator from local measurements of the active and reactive powers at the output of each unit.

Primary control makes it possible to solve the problem of the physical disparity between the distributed generators, to dampen the transient state during the connection and the disconnection of the generators and to avoid the appearance of circulating currents, which can bring the system to instability. This level of control generates slight variations on the voltage's frequency and amplitude, hence the need for secondary control.[2]

I.8.3 Secondary control

Secondary control is intended to restore the frequency and voltage amplitude to their nominal values. Indeed, during the application of the primary control to correctly share the powers, the frequency and the amplitude of the reference voltages of each generation unit vary according to the droop laws used. These variations generate a deviation of the operating point of the system from its nominal position and may exceed the allowable margins established by international standards, i.e. a margin of 2% for the frequency and a margin of 5% for the voltage amplitude (Standard NF EN 50160)[2]. The secondary control acts to restore the nominal values of the frequency and amplitude of voltage using the information collected through the use of means of communication between the different distributed generation units. The compensation of deviations produced by the primary control is therefore ensured by the higher level of control.

I.8.4 Tertiary control

This type of control is mainly applied to microgrid and distributed generators connected to the distribution grid. It requires devices and strategies of communication (centralized or decentralized) to control power flows between the microgrid on one hand and the distribution network on the other.

This control corresponds to the highest hierarchical level and operates with a very slow dynamics. It is applied mainly for systems connected to the distribution grid. This level of control also makes it possible, depending on the economic objectives, to ensure optimal operation of the microgrid and to manage the power flows between the microgrid and the main grid. In the grid-connected mode, power flow can be managed by adjusting the amplitude and frequency of distributed generators.[15]

In the remaining of this chapter, we focus on the first two levels of control, namely the primary control and the level-zero control dedicated to the regulation of the voltage or the current. These two levels and the secondary control are the three main levels treated in this work. Several control techniques have been used in the literature. These techniques are presented in figure I.6.

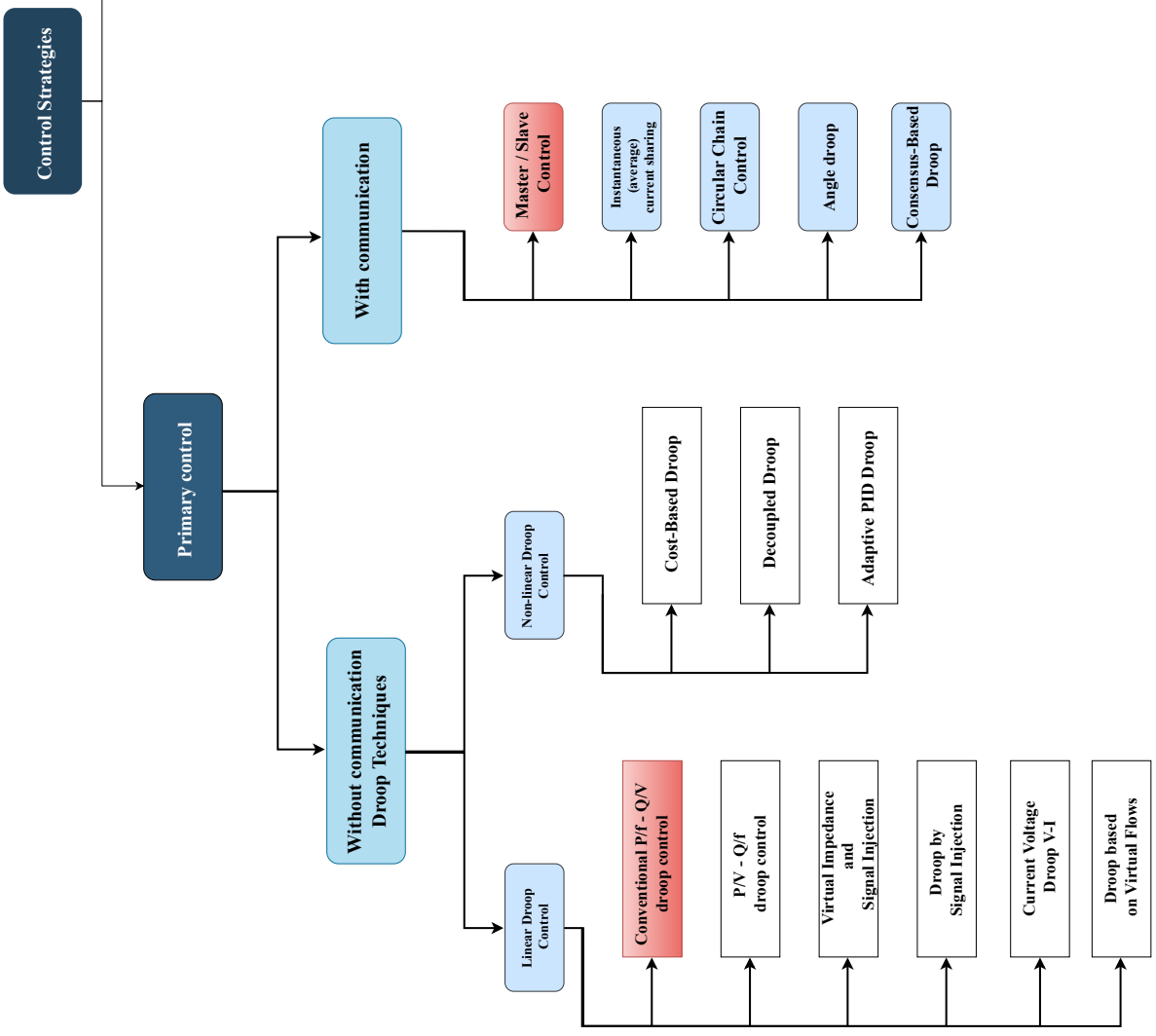

Figure I.6: Classification of local control methods applied to distributed generation systems[2]

I.9 Internal control (Level zero)

In this level, several methods have been used in literature such as classic, nonlinear, predictive, learning-based and robust control as we have seen in figure I.6. In this work, we have chosen to use sliding mode control thanks to its advantages.

Sliding mode control:

Sliding mode control is a nonlinear control that has been used on distributed generation systems. This easy-to-implement control provides good disturbance rejection and low sensitivity to parametric variations on the system.

I.10 Primary control:

Primary control ensures the sharing of power flows between the various distributed generators. This sharing can be ensured by centralized and decentralized control techniques. This control is added to the internal control, responsible for voltage regulation, to ensure that an equitable distribution of loads and power flows is maintained in microgrids made up of several distributed generation units.

I.10.1 Centralized primary control :

The centralized primary control of power sharing mainly focuses on the collection of information and measurements via means of communication. This control is based on centralized decision-making, which imposes communications for the transmission and reception of measurement and command signals. Several centralized techniques have been proposed in the literature to ensure power sharing. Among these techniques: the master-slave technique, the instantaneous (average) current sharing technique, the circular chain technique, the angular droop control as well as the consensus-based droop control. In this work we will use one of these methods which is master/slave control and more specifically master/slave control with central controller.

1. Master/slave control with central controller : It is one of the variants of master-slave control method. It is similar to the methods used for paralleling DC/DC converters. In this method, one of the inverters operates in the voltage control mode (the master / forming) and all the others (the slaves) operate in current-mode control (following) [4]. A basic system structure representing one phase is shown in Figure I.7.

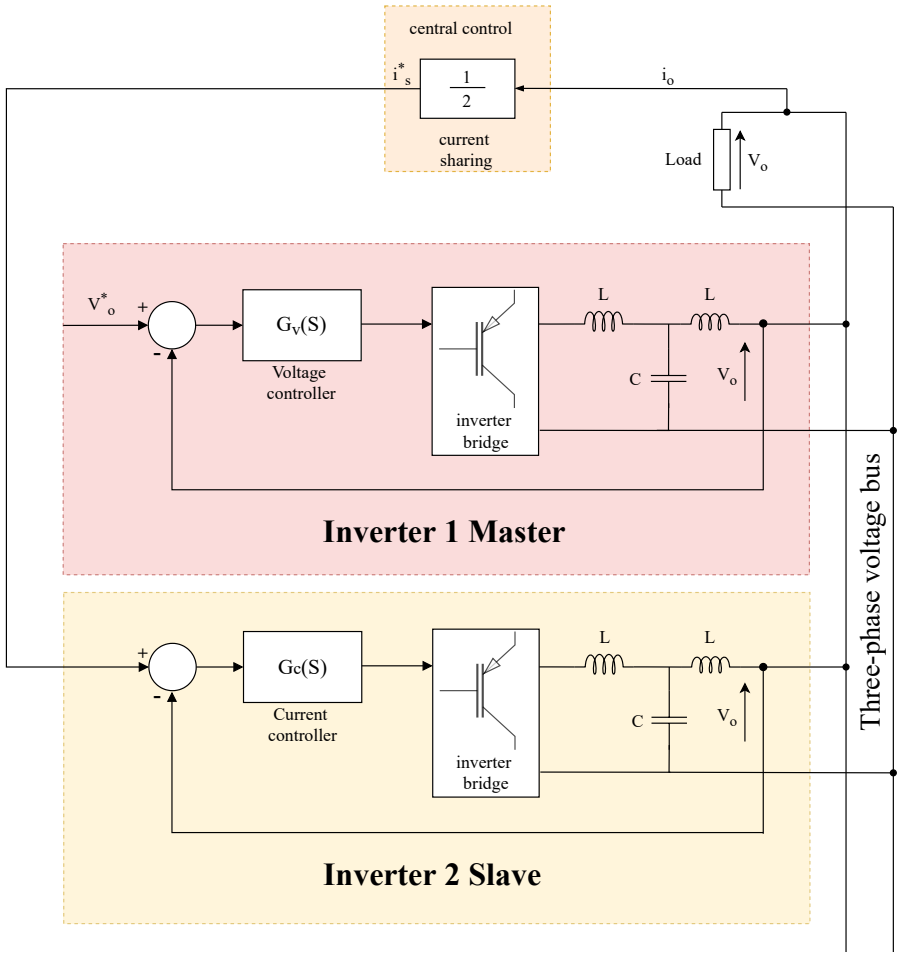

Figure I.7: Master/slave control principle with central controller [4]

There is only one shared signal between the converters in this method, it is the slave reference current i_s^*. The current sharing block generates this signal from the measured load current i_o, by dividing it by the number of converters connected to the system N. The output voltage vo of the system is controlled from the master unit, by using the voltage controller $G_v(s)$, and the slave units have to provide the current demanded by the load. The role of the current controller $G_c(s)$ is to decrease the difference between the reference slave current i_s^* and the actual slave currents.

I.10.2 Decentralized primary control :

Decentralized primary control techniques are mainly based on droop techniques. These techniques are used to deal with the difficulties associated with the use of the means of communication in centralized primary control structures.[2] in this level of control there are many techniques that have been used as we have seen in figure I.6. In this work, we will use the conventional P/f-Q/V droop control.

Conventional P/f-Q/V droop control :

The conventional droop control technique allows the different distributed generators existing in a microgrid to share the power demanded by the loads. It is a technique based on power theory that allows distributed generation systems to emulate the behaviour of a synchronous generator by giving it a kind of virtual inertia. The principle of this technique is shown in Figure I.8.

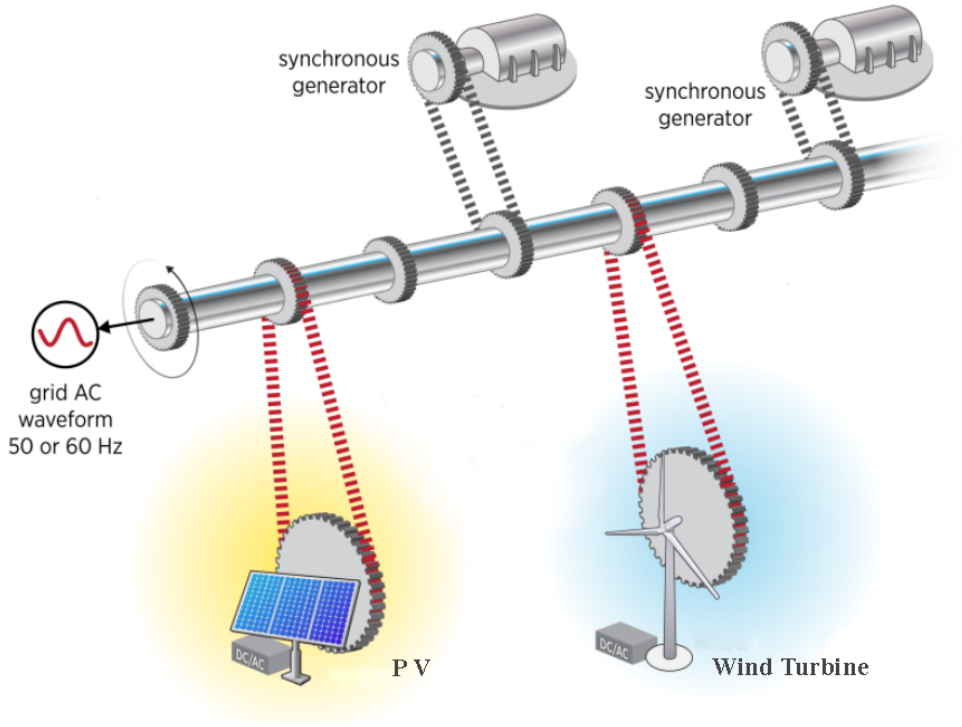

Figure I.8: Virtual inertia emulation for low inertia generators [2]

In conventional synchronous generators, the regulation of the active power is linked to the rotation speed of the generator and that of the reactive power is linked to the amplitude of the (emf). This approach is transferred to conventional droop control by making the analogy between conventional generation systems and distributed generators based on renewable energies as presented in Figure I.9. Beyond that, the variation in the flows of active and reactive powers is now a function of the amplitude and frequency of the output voltage of each distributed generator. Beyond that, the variation in the flows of active and reactive powers is now a function of the amplitude and frequency of the output voltage of each distributed generator. This equivalence made it possible to improve the sharing of power flows and to reinforce stability by bringing back a kind of virtual inertia to the system. In addition to virtual inertia, this technique ensures compatibility by unifying the control applied to both renewable energy-based systems and conventional synchronous systems.

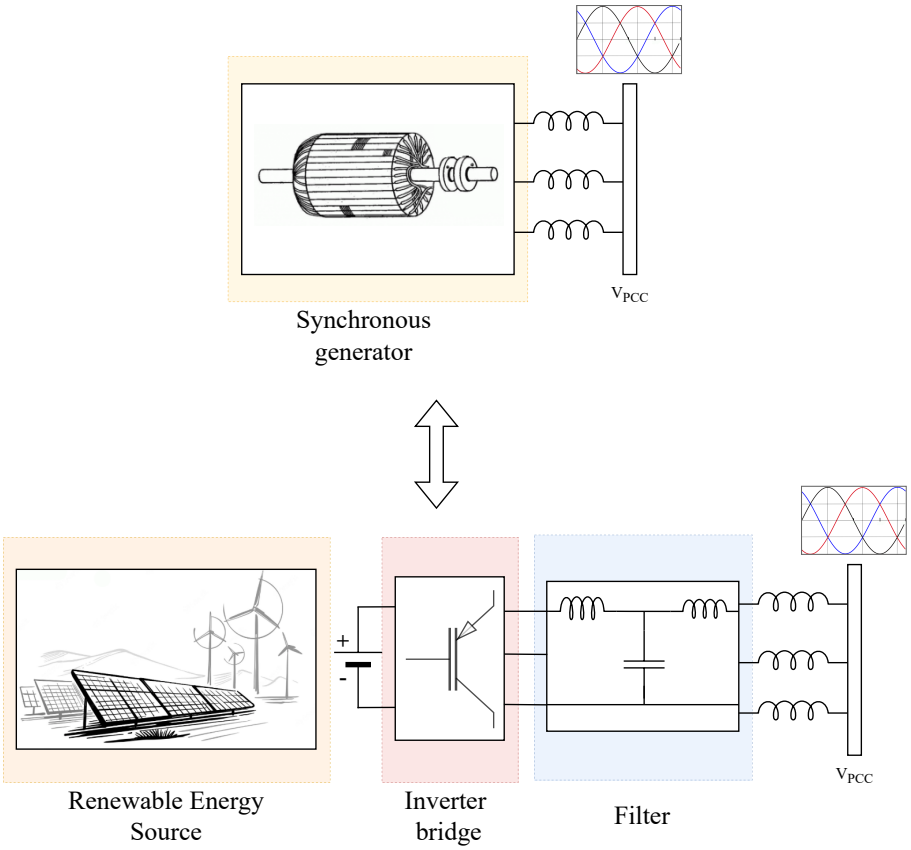

Figure I.9: Analogy between conventional generation systems and distributed generation systems based on renewable energies[2]

These characteristics make it possible to support the decentralization of electricity generation systems by allowing them to operate autonomously in remote rural areas with very large distances separating the generation units from the consumers.

1. Stand-alone microgrid model:

   The structure of a standalone microgrid can be described by Figure I.10 :

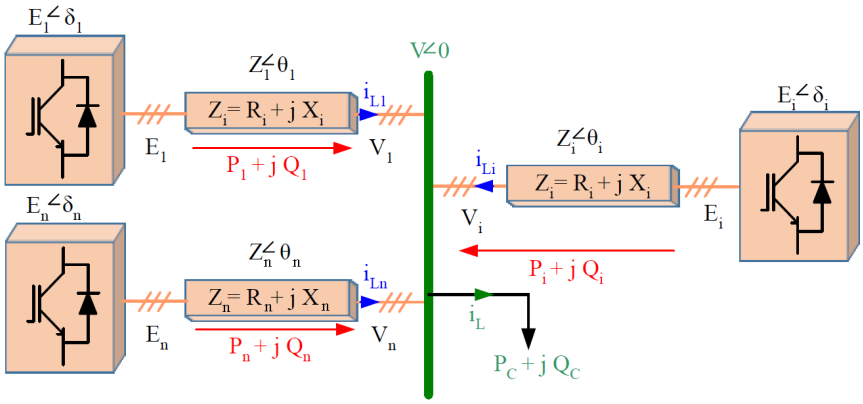

Figure I.10: Electrical model of a standalone microgrid

In this representation of the autonomous microgrid, each distributed generation unit is modeled by a Thevenin generator. A model composed of an ideal voltage source of amplitude E_i and internal angle δ_i in series with output impedance "Z_i". This output impedance includes both the internal impedance of the generator, the impedance of the filter at the output as well as a line impedance ensuring the connection of each elementary DG to the PCC. The voltages and currents at the output of each distributed generator are denoted by V_i and I_{L_i} respectively.

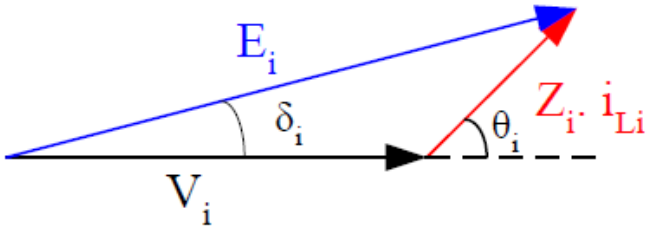

Figure I.11: Vector diagram of the voltages of an elementary distributed generator

$$V_i(p) = E_i(p) - Z_i(p) I_{Li}(p) \tag{I.3}$$

The determination of the power expressions supplied by each elementary DG with index "i" to the loads locally installed on the PCC bus results from the expression of its complex apparent power given by:

$$S_i = V_i I_{Li}^* = V_i \left(\frac{E_i - V_i}{Z_i} \right)^* = P_i + jQ_i \tag{I.4}$$

Or $V_i = V$

$$S_i = V \left(\frac{E_i - V_i}{Z_i} \right)^* = P_i + jQ_i \tag{I.5}$$

Based on the previous equation (I.5), the expressions for the active transmitted powers P_i and reactive Q_i are described by equations (I.6) and (I.7) respectively.

$$P_i = \frac{V}{Z_i} \left[(E_i \cos \delta_i - V) \cos \theta_i + E_i \sin \delta_i \sin \theta_i \right] \tag{I.6}$$

$$Q_i = \frac{V}{Z_i} \left[(E_i \cos \delta_i - V) \sin \theta_i - E_i \sin \delta_i \cos \theta_i \right] \tag{I.7}$$

Where, $Z_i = R_i + jX_i$ output impedance of each DGi characterized by a phase angle θ_i which corresponds to the phase angle between the voltage at the output of each elementary

generator of index "i" and the voltage "V" at the PCC load bus.
Equations (I.6) and (I.7) show that, similar to synchronous generators, power distribution is controlled by means of physical variables specific to each generation unit (voltage and phase shift angle). Moreover, this power distribution is related to the output Z_i and their character (inductive, resistive or capacitive). A character which mainly depends on the parameters of the filter at the output, the line impedance which influences the choice of the control strategy to be used. Depending on the predominance of the output impedance of each DG, different variants of classic droop controls can be used.

1. Case 1. Inductive impedance ($\theta = 90°$) :
In the microgrid where each distributed generation unit is characterized by a sufficiently low R_i/X_i ratio, the output impedance is considered to be predominantly inductive. This situation corresponds to medium and high voltage grids which supply very distant loads. Under these conditions, the active and reactive power equations already expressed in (I.6) and (I.7) can be simplified to give equations (I.8) and (I.9).

$$P_i = \frac{VE_i}{L\omega_i}\sin(\delta_i) \tag{I.8}$$

$$Q_i = \frac{V}{L\omega_i}\left(E_i\cos\delta_i - V\right) \tag{I.9}$$

In the case where the internal generator angle is very small δ_i which is always the case: (less than 0.1rad) this leads to the following mathematical simplifications: $\sin(\delta_i) = \delta_i$ and $\cos(\delta_i) = 1$ Consequently, the equations (I.8) and (I.9) can be further simplified to have the expressions (I.10) and (I.11):

$$P_i = \frac{VE_i}{L\omega_i}\delta_i \tag{I.10}$$

$$Q_i = \frac{V}{L\omega_i}\left(E_i - V\right) \tag{I.11}$$

Where

$$\delta_i = \int 2\pi f_i = \int \omega_i \tag{I.12}$$

By deriving equations (I.10) and (I.11), this gives

$$\begin{cases} \dfrac{\partial P_i}{\partial E_i} = \dfrac{V}{L\omega_i}\delta_i \\ \dfrac{\partial P_i}{\partial \delta_i} = \dfrac{VE_i}{L\omega_i} \end{cases} \quad \& \quad \begin{cases} \dfrac{\partial Q_i}{\partial E_i} = \dfrac{V}{L\omega_i} \\ \dfrac{\partial Q_i}{\partial \delta_i} = 0 \end{cases} \tag{I.13}$$

Equations (I.9), (I.10) as well as (I.13) prove that active and reactive powers can be regulated separately. Indeed, the active power depends on the internal angle δ_i and it can be adjusted accordingly by the variation of this angle. Reactive power, on the other hand, depends directly on the amplitude of the voltage E_i. These findings present the origin of the basic idea of droop control. Consequently, to ensure power sharing between parallel distributed generators, the use of droop characteristics relating active power to frequency (P-ω) and reactive power to voltage amplitude (Q-E) is recommended. For these characteristics, the reference voltages to be applied to each DGi have E_i as their amplitude and oscillate at the frequency ω_i These quantities are determined by expressions (I.14) and (I.15) of classical droop for an inductive behaviour.

$$\omega_i = \omega_0 - m_p \left(P_i - P^*\right) \tag{I.14}$$

$$E_i = E_0 - n_q \left(Q_i - Q^*\right) \tag{I.15}$$

Where P_i and Q_i represent respectively the active and reactive powers at the output of each converter. ω_i and E_i represent the pulsation and the RMS value of the reference voltage. Respectively, P^* and Q^* are the nominal active and reactive powers respectively. K_{p_i} and K_{i_i} are the droop coefficients for the frequency and the voltage, which are chosen according to the nominal active and reactive powers.

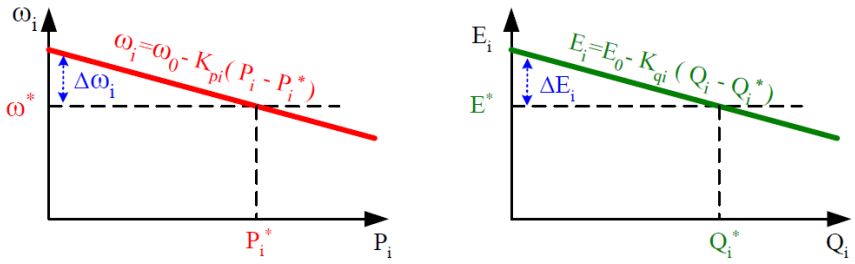

Figure I.12: Droop curve for a system with inductive behaviour [2]

For more clarity on conventional droop control for an inductive microgrid, the control diagram based on equations (I.14) and (I.15) can be summarized in Figure I.13.

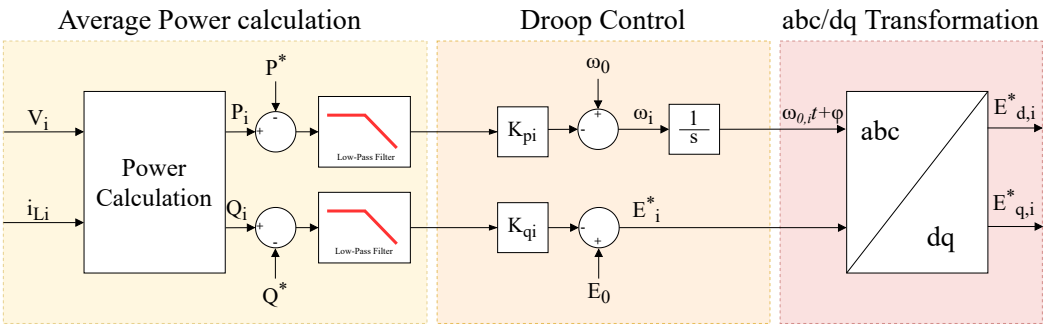

Figure I.13: Block diagram of conventional droop control, for inductive output impedance [5]

2. Case 2. Resistive impedance (θ=0°) :
   At low voltage, the output impedance of each converter have a resistive nature and the R_i/X_i ratio becomes high to a point where the impedance phase shift angle can be considered zero ($\theta = 0°$). Under these conditions, equations (I.7) and (I.8) are written differently as follows:

$$P_i = \frac{V}{R_i}\left(E_i \cos\delta_i - V\right) \tag{I.16}$$

$$Q_i = -\frac{VE_i}{L\omega}\sin\delta_i \tag{I.17}$$

   The internal angle δ is very small, which makes it possible to simplify equations (I.16) and (I.7) until it yields :

$$P_i = \frac{VE_i}{R_i} - \frac{V^2}{R_i} \tag{I.18}$$

$$Q_i = -\frac{VE_i}{L\omega}\delta_i \tag{I.19}$$

   The derivation of equations (I.18) and (I.19) gives :

$$\begin{cases} \dfrac{\partial P_i}{\partial E_i} = \dfrac{V}{R_i} \\ \dfrac{\partial P_i}{\partial \delta_i} = 0 \end{cases} \quad \& \quad \begin{cases} \dfrac{\partial Q_i}{\partial E_i} = -\dfrac{V}{L\omega_i}\delta_i \\ \dfrac{\partial Q_i}{\partial \delta_i} = -\dfrac{VE_i}{L\omega} \end{cases} \tag{I.20}$$

   As it should be noticed, from equations (I.18), (I.19) and (I.20) it is clear that the active power P_i is related to the amplitude of the voltage of the DGi and that the flow of the reactive power is dependent on the internal angle δ_i. These findings lead to the conclusion that the active power can be regulated by the amplitude of the voltage. While the reactive power is regulated by the angle δ_i. Under these conditions, the use of droop equations relating active power to voltage amplitude (P-E) and reactive power to frequency (Q-ω) is recommended.

3. Calculation of droop coefficients :

In the context of distributed generation microgrids, the droop equations (I.14), (I.15) behave like a virtual communication agent that watches over the correct sharing of power between the different distributed generators. To achieve this, the droop control must limit variations in the amplitude and frequency of the voltage at the output of each distributed generation unit. Variations controlled and limited by IEEE Std 1547-2018[2]. According to this standard, the percentage of the variation of the nominal voltage is limited to ±5% of its nominal value, while that of the frequency is limited to ±1%. By following the requirements of the standards, it should be noted that the deviations on the amplitude of the voltage and on the output frequency must be limited to an acceptable interval defined by

$$\begin{cases} |\omega_i - \omega_0| \leq \Delta\omega_{i\,\max} \\ |E_i - \omega_0| \leq \Delta E_{i\,\max} \end{cases} \tag{I.21}$$

Where $\Delta\omega_{max}$ and ΔE_{max} represent the maximum allowed limits for the pulse frequency and for the voltage amplitude variation respectively. From the standards and authorized limits, the droop coefficients can be calculated either for a P-ω /Q-E or P-E/Q-ω droop control. The droop coefficients for the P-ω/Q-E characteristics can be determined as follows:

$$K_{pi} = \frac{\omega_{\text{imax}} - \omega_{\text{imin}}}{P_{\text{imax}} - P_{\text{imin}}} = \frac{\Delta\omega_{\text{imax}}}{\Delta P_{\text{imax}}} \tag{I.22}$$

$$K_{qi} = \frac{E_{\text{imax}} - E_{\text{imin}}}{Q_{\text{imax}} - Q_{\text{imin}}} = \frac{\Delta E_{\text{imax}}}{\Delta Q_{\text{imax}}} \tag{I.23}$$

Whereas in the droop case that follows the P-E/Q-ω characteristics, these parameters are determined as follows:

$$C_{pi} = \frac{E_{i\,\max} - E_{i\,\min}}{P_{i\,\max} - P_{i\,\min}} = \frac{\Delta E_{i\,\max}}{\Delta P_{i\,\max}} \tag{I.24}$$

$$C_{qi} = \frac{\omega_{i\,\max} - \omega_{i\,\min}}{Q_{i\,\max} - Q_{i\,\min}} = \frac{\Delta\omega_{i\,\max}}{\Delta Q_{i\,\max}} \tag{I.25}$$

Where $P_{i,max}$ and $Q_{i,max}$ are respectively the maximum active and reactive powers and which are often equal to the nominal powers of each DGi. $P_{i,min}$ and $Q_{i,min}$ are also the minimum active and reactive powers of each DGi often taken equal to zero. ω_{imax}, ω_{imin} and $E_{i,max}$,$E_{i,min}$ are respectively the minimum and maximum pulsations as well as the maximum and minimum amplitudes authorized according to the international standard.

I.11 Conclusion

As we have seen in this first chapter, we got more familiar with the term "microgrid" and its modes of operation, we have also presented the DC-AC converters (inverters), their classification and their use in a parallel-connected scenario.

We have also seen the different stages and strategies for controlling a microgrid, namely the internal and primary control strategies. In the next chapter, we will discuss the implementation of the latter control strategies, more specifically, using sliding mode technique for the internal control and the conventional P-f Q-V droop control for the decentralized primary control as well as the master/slave control with a central controller as a centralized primary control.

In this work we will focus on islanded microgrids, so the tertiary control isn't needed, but it has to be noted that in the case of a connection to the grid, it is required to have a Phase-Locked Loop (or PLL) in order to match the phase between the output of a microgrid and the traditional grid.[16][17]

Chapter II

Models and Tools

II.1 Introduction

The key to design a good and robust control law that implicates a system to follow a certain desired behaviour is to first, obtain a mathematical model that can accurately describe a system's exact behaviour to a certain degree, then to design a control law that allows this system to achieve whatever objective we have in mind for it. In this chapter, we will focus on modelling our inverter so that we can in a second part, focus on choosing a control law that adequately conforms to our specifications.

II.2 Inverter's Modelling

An inverter is a power device that can be subdivided into two major parts as shown in Figure II.1: the inverter's bridge and the LCL filter. Each of the two parts has its mathematical model that expresses the relationship between the inputs and the outputs.

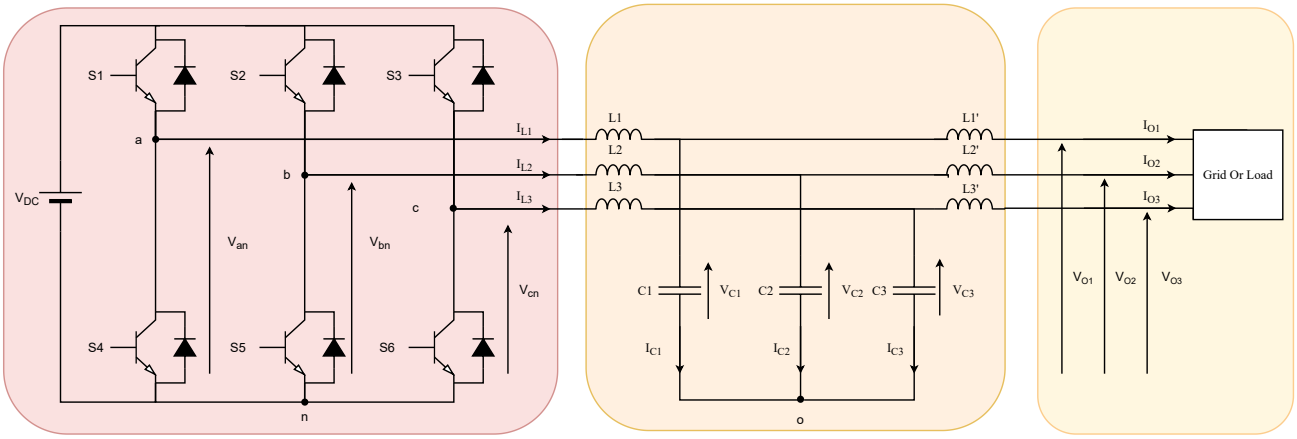

Figure II.1: Inverter's bridge and a LCL filter

A good model of our inverter can describe its dynamics and make predictions about its behaviour in a way that can permit to implement a control law and simulate its functioning.

II.2.1 Inverter's bridge model

An inverter's bridge model is established by making some assumptions that are sufficiently accurate so as not to affect the validity of the used model such as [18]:

- Switching and conduction losses are negligible to our research, in this case, all semiconductor switches become ideal or perfect switches, in other words they behave as zero value resistance in their ON-state and as a infinite value on their OFF-state.
- Generators are considered perfect, in the sense that an ideal voltage source is considered to have no internal resistance and provide a constant value of voltage at any time and regardless the current it delivers.
- Passive elements are considered linear and invariant.

In this work, we will be using a three-phase two-level inverter as show in the figure II.2:

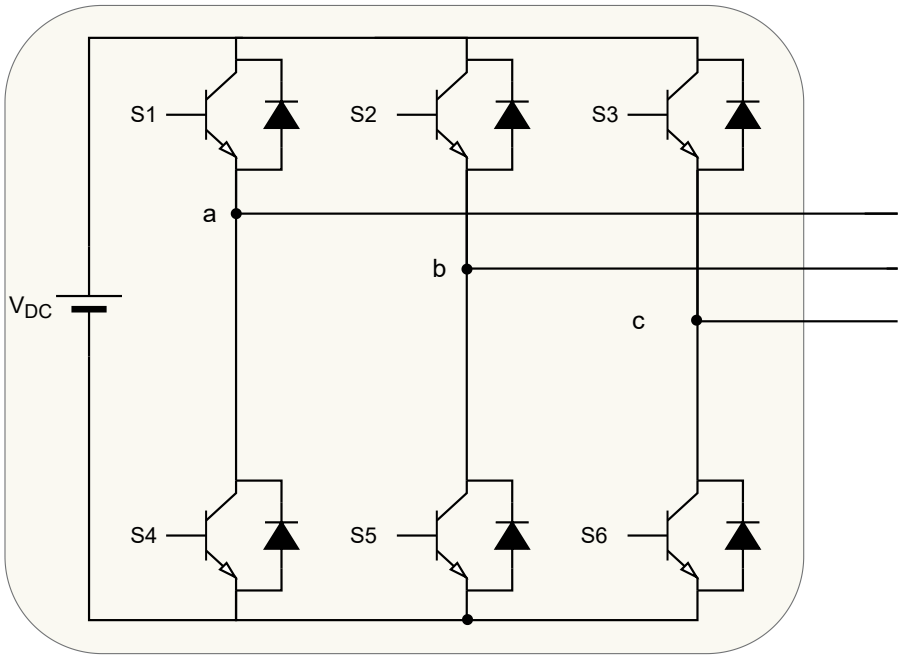

Figure II.2: Inverter's bridge

As we can see in figure II.2 our inverter is composed of six total switches. It has to be noted that each two switches sharing a "leg", for example S1 and S4 are always complementary switched, meaning they cannot be both open or both closed at the same time. Taking that into consideration, and by using Kirchhoff's law, we can describe the relationship between the

phase-to-neutral voltages (V_{an} ,V_{bn} ,V_{cn}) and the upper switches (S1, S2, S3) with the following equation:

$$\begin{bmatrix} V_{an} \\ V_{bn} \\ V_{cn} \end{bmatrix} = \frac{1}{3} V_{dc} \begin{bmatrix} 2 & -1 & -1 \\ -1 & 2 & -1 \\ -1 & -1 & 2 \end{bmatrix} \cdot \begin{bmatrix} S1 \\ S2 \\ S3 \end{bmatrix} \tag{II.1}$$

II.2.2 LCL Filter Modelling

To test our control models, an LCL filter model is established, in Figure II.3, a three-legged LCL filter is shown, which mainly consists of a set of three-phase inductors, a set of three-phase capacitors and another set of three-phase inductors

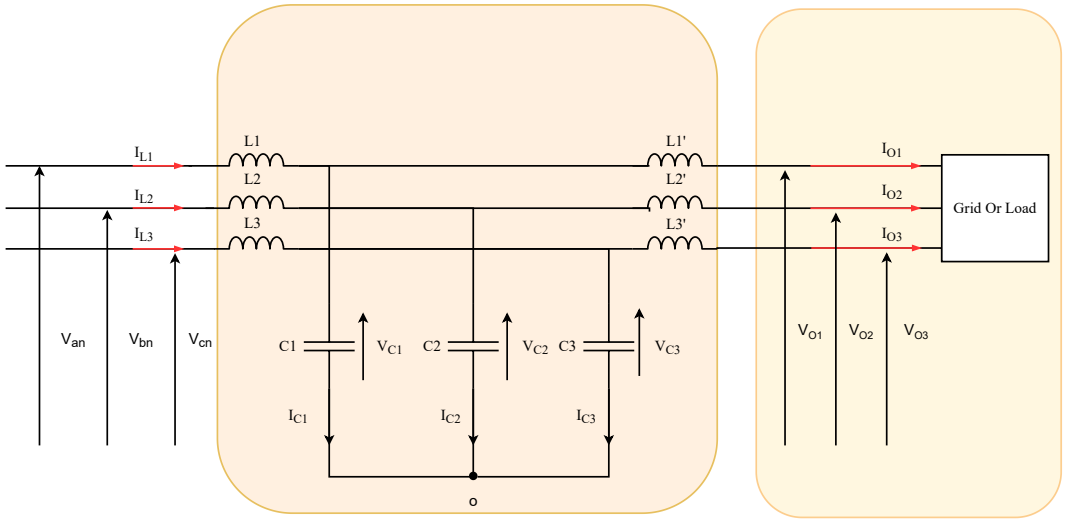

Figure II.3: LCL filter model

We are going to divide the modelling of the LCL filter into three parts :

- In the First part we handle the currents of the first set of inductors
- The second part will be about the voltage of the capacitors
- The third part manages the currents of the second set of the inductors

It has to be noted that in our model and from the assumptions that are made later on, the order of the system is reduced from a model that contains nine states, namely are:

- Three currents of the first set of inductors.
- Three voltages of the capacitors.
- Three currents of the second set of inductors.

To a model that contains only six states. So to begin describing the system's dynamics and by using Kirchhoff's law we find:

$$\begin{cases} V_{an} - L_1\dot{I}_{L1} - V_{C1} + V_{C2} + L_2\dot{I}_{L2} - V_{bn} = 0 \\ V_{bn} - L_2\dot{I}_{L2} - V_{C2} + V_{C3} + L_3\dot{I}_{L3} - V_{cn} = 0 \end{cases} \tag{II.2}$$

$$\begin{cases} L_1\dot{I_{L1}} - L_2\dot{I_{L2}} = -V_{C1} + V_{C2} + V_{an} - V_{bn} \\ L_2\dot{I_{L2}} - L_3\dot{I}_{L3} = -V_{C2} + V_{C3} + V_{bn} - V_{cn} \end{cases} \tag{II.3}$$

From the neutral point (or the node "o"), we can find:

$$I_{C1} + I_{C2} + I_{C3} = 0 \tag{II.4}$$

And from the upper nodes, we find that:

$$I_{Ci} = I_{Li} - I_{Oi}\ ; \qquad i = 1, 2, 3 \tag{II.5}$$

Which means that:

$$I_{L1} + I_{L2} + I_{L3} - (I_{O1} + I_{O2} + I_{O3}) = 0 \tag{II.6}$$

By making the assumption of a physical constraint being applied on the output currents which is a neutral point being present in the connection of the load (meaning that the load is connected in a star or Y form), the output currents can be described as the following :

$$I_{O1} + I_{O2} + I_{O3} = 0 \tag{II.7}$$

After the assumption being made in (II.7), we find that:

$$I_{L1} + I_{L2} + I_{L3} = 0 \tag{II.8}$$

By differentiation (II.8) we find:

$$\dot{I_{L1}} + \dot{I_{L2}} + \dot{I_{L3}} = 0 \tag{II.9}$$

That means that :

$$\dot{I_{L3}} = -\left(\dot{I_{L1}} + \dot{I_{L2}}\right) \tag{II.10}$$

By replacing equation (II.10) in II.3 we find:

$$\begin{cases} L_1\dot{I_{L1}} - L_2\dot{I_{L2}} = -V_{C1} + V_{C2} + V_{an} - V_{bn} \\ L_3\dot{I_{L1}} + (L_2 + L_3)\,\dot{I_{L2}} = -V_{C2} + V_{C3} + V_{bn} - V_{cn} \end{cases} \tag{II.11}$$

From the figure II.3, we can deduce:

$$\begin{cases} V_{an} = S1V_{DC} \\ V_{bn} = S2V_{DC} \\ V_{cn} = S3V_{DC} \end{cases} \tag{II.12}$$

So

$$V_{an} - V_{bn} = (S1 - S2)V_{DC} \tag{II.13}$$

$$V_{bn} - V_{cn} = (S2 - S3)V_{DC} \tag{II.14}$$

Returning to the assumption made for the equation (II.7), a software condition that states :

$$S1 + S2 + S3 = \frac{3}{2} \tag{II.15}$$

is optimal in the sense that:

- It guarantees the symmetry of the duty cycles in balanced cases (centered around 0.5 and regularly shifted).
- It results in a voltage V_{no} equal to $\frac{V_{DC}}{2}$ Which makes the inverter emulate the operation of a two-source inverter with mid-point.
- It maximizes admissible space of the load currents.

We are looking for $S3$ so :

$$\mathrm{S3} = \frac{3}{2} - (\mathrm{S1} + \mathrm{S2}) \tag{II.16}$$

So (II.14) becomes :

$$V_{bn} - V_{cn} = \left(S1 + 2S2 - \frac{3}{2}\right) V_{DC} \tag{II.17}$$

by replacing equations (II.13) and (II.17) in (II.11) we find:

$$\begin{cases} L_1\dot{I_{L1}} - L_2\dot{I_{L2}} = -V_{C1} + V_{C2} + (S1 - S2)V_{DC} \\ L_3\dot{I_{L1}} + (L_2 + L_3)\,\dot{I_{L2}} = -V_{C2} + V_{C3} + \left(S1 + 2.S2 - \frac{3}{2}\right) V_{DC} \end{cases} \tag{II.18}$$

Coming back to equation (II.4) and by replacing

$$I_{Ci} = C_i\dot{V_{Ci}} \; ; \qquad i = 1, 2, 3 \tag{II.19}$$

We can find the following :

$$C_1\dot{V_{C1}} + C_2\dot{V_{C2}} + C_3\dot{V_{C3}} = 0 \tag{II.20}$$

And this means that:

$$\dot{V_{C3}} = -\frac{C_1}{C_3}\dot{V_{C1}} - \frac{C_2}{C_3}\dot{V_{C2}} \tag{II.21}$$

By integrating (II.21) and considering that the capacitors are initially discharged we find :

$$V_{C3} = -\frac{C_1}{C_3}V_{C1} - \frac{C_2}{C_3}V_{C2} \tag{II.22}$$

By replacing equation (II.22) in (II.18)

$$\begin{cases} L_1\dot{I_{L1}} - L_2\dot{I_{L2}} = -V_{C1} + V_{C2} + (S1 - S2)V_{DC} \\ L_3\dot{I_{L1}} + (L_2 + L_3)\,\dot{I_{L2}} = -\frac{C_1}{C_3}V_{C1} + -(\frac{C_2}{C_3} + 1)V_{C2} + S1V_{DC} + 2.S2V_{DC} - \frac{3}{2}V_{DC} \end{cases} \tag{II.23}$$

For the second part of the modelling,the objective is to find the dynamics of the capacitor's voltages, from the equation (II.5) we have:

$$\begin{cases} I_{C1} = I_{L1} - I_{O1} \\ I_{C2} = I_{L2} - I_{O2} \end{cases} \tag{II.24}$$

By replacing (II.19) in (II.24), we obtain:

$$\begin{cases} C_1\dot{V_{C1}} = I_{L1} - I_{O1} \\ C_2\dot{V_{C2}} = I_{L2} - I_{O2} \end{cases} \tag{II.25}$$

Or

$$\begin{cases} \dot{V_{C1}} = \frac{1}{C_1}I_{L1} - I_{O1} \\ \dot{V_{C2}} = \frac{1}{C_2}I_{L2} - I_{O2} \end{cases} \tag{II.26}$$

In addition, for the third part, the second set of inductors, and by using kirchoff's law we find:

$$\begin{cases} V_{O1} + L_1'\dot{I}_{O1} - V_{C1} = 0 \\ V_{O2} + L_2'I_{O2} - V_{C2} = 0 \end{cases} \tag{II.27}$$

The expression of the output currents becomes as follows:

$$\begin{cases} \dot{I_{O1}} = \frac{1}{L_1'}V_{C1} - \frac{1}{L_1'}V_{O1} \\ \dot{I_{O2}} = \frac{1}{L_2'}V_{C2} - \frac{1}{L_2'}V_{O2} \end{cases} \tag{II.28}$$

For the third output current I_{O3}, adding its equation is unnecessary since the assumption made in equation (II.7) is established. Finally, by summing up equations (II.23), (II.26) and

(II.28), the system's dynamics can be described by the following :

$$\begin{cases} L_1\dot{I_{L1}} - L_2\dot{I_{L2}} = -V_{C1} + V_{C2} + S1V_{DC} - S2V_{DC} \\ L_3\dot{I_{L1}} + (L_2 + L_3)\,\dot{I_{L2}} = -\frac{C_1}{C_3}V_{C1} - \left(\frac{C_2}{C_3} + 1\right)V_{C2} + S1V_{DC} + 2.S2V_{DC} - \frac{3}{2}V_{DC} \\ \dot{V_{C1}} = \frac{1}{C_1}I_{L1} - \frac{1}{C_1}I_{O1} \\ \dot{V_{C2}} = \frac{1}{C_2}I_{L2} - \frac{1}{C_2}I_{O2} \\ \dot{I_{O1}} = \frac{1}{L'_1}V_{C1} - \frac{1}{L'_1}V_{O1} \\ I_{O2} = \frac{1}{L'_2}V_{C2} - \frac{1}{L'_2}V_{O2} \end{cases} \tag{II.29}$$

By taking :

$$L_1 = L_2 = L_3 = L$$
$$C_1 = C_2 = C_3 = C$$

We get :

$$\begin{cases} L\dot{I_{L1}} - L\dot{I_{L2}} = -V_{C1} + V_{C2} + S1V_{DC} - S2V_{DC} \\ L\dot{I_{L1}} + 2L\dot{I_{L2}} = -V_{C1} - 2V_{C2} + S1V_{DC} + 2 \cdot S2V_{DC} - \frac{3}{2}V_{DC} \\ \dot{V_{C1}} = \frac{1}{C}I_{L1} - \frac{1}{C}I_{O1} \\ \dot{V_{C2}} = \frac{1}{C}I_{L2} - \frac{1}{C}I_{O2} \\ \dot{I_{O1}} = \frac{1}{L'}V_{C1} - \frac{1}{L'}V_{O1} \\ \dot{I}_{O2} = \frac{1}{L'}V_{C2} - \frac{1}{L'}V_{O2} \end{cases} \tag{II.30}$$

By simplifying the first and second equation of (II.30), we get :

$$\text{‘} \begin{cases} \dot{I_{L1}} = -\frac{1}{L}V_{C1} + \frac{V_{DC}}{L}S1 - \frac{V_{DC}}{2L} \\ \dot{I_{L2}} = -\frac{1}{L}V_{C2} + \frac{V_{DC}}{L}S2 - \frac{V_{DC}}{2L} \\ \dot{V_{C1}} = \frac{1}{C}I_{L1} - \frac{1}{C}I_{O1} \\ \dot{V_{C2}} = \frac{1}{C}I_{L2} - \frac{1}{C}I_{O2} \\ \dot{I_{O1}} = \frac{1}{L'}V_{C1} - \frac{1}{L'}V_{O1} \\ \dot{I_{O2}} = \frac{1}{L'}V_{C2} - \frac{1}{L'}V_{O2} \end{cases} \tag{II.31}$$

If we chose:

$$X = \begin{bmatrix} I_{L1} \\ I_{L2} \\ V_{C1} \\ V_{C2} \\ I_{O1} \\ I_{O2} \end{bmatrix}; U1 = \begin{bmatrix} S1 \\ S2 \end{bmatrix}; U2 = \begin{bmatrix} V_{O1} \\ V_{O2} \end{bmatrix} \tag{II.32}$$

With X being the state vector, $U1$ and $U2$ being the input vectors ($U1$ is our control vector and $U2$ elements are considered as measurable disturbances). A state space representation can describe our system's dynamics:

$$\dot{X} = \begin{bmatrix} 0 & 0 & -\frac{1}{L} & 0 & 0 & 0 \\ 0 & 0 & 0 & -\frac{1}{L} & 0 & 0 \\ \frac{1}{C} & 0 & 0 & 0 & -\frac{1}{C} & 0 \\ 0 & \frac{1}{C} & 0 & 0 & 0 & -\frac{1}{C} \\ 0 & 0 & \frac{1}{L'} & 0 & 0 & 0 \\ 0 & 0 & 0 & \frac{1}{L'} & 0 & 0 \end{bmatrix} X + \begin{bmatrix} \frac{V_{DC}}{L} & 0 \\ 0 & \frac{V_{DC}}{L} \\ 0 & 0 \\ 0 & 0 \\ 0 & 0 \\ 0 & 0 \end{bmatrix} U1 + \begin{bmatrix} 0 & 0 \\ 0 & 0 \\ 0 & 0 \\ 0 & 0 \\ -\frac{1}{L'} & 0 \\ 0 & -\frac{1}{L'} \end{bmatrix} U2 + \begin{bmatrix} -\frac{V_{DC}}{2L} \\ -\frac{V_{DC}}{2L} \\ 0 \\ 0 \\ 0 \\ 0 \end{bmatrix} \tag{II.33}$$

As we have mentioned before, even though that $U2$ is considered to be a disturbance, a robust control implementation should reject the effect of the disturbance on the regulated variables.

II.2.3 PID Controller

The PID controller is the most used technique in the control of industrial processes. The major reasons for its wide acceptance in industry are its ability to control the majority of processes, its actions that are well understood and its implementation that is relatively simple. The design and tuning of the PID controller has been a subject of research since the day Ziegler and Nichols presented their tuning method in 1942[19]. Although there are several techniques for tuning PID controller parameters.

Tuning a control loop is arranging the control parameters to their optimum values in order to obtain desired control response. At this point, stability is the main necessity, but beyond that, different systems lead to different behaviours and requirements and these might not be compatible with each other. In principle, PID tuning seems completely easy, consisting of only three parameters, however, in practice; it is a difficult problem because the complex criteria at the PID limit should be satisfied. PID tuning is mostly a heuristic concept but existence of many objectives to be met such as short transient, high stability makes this process harder. Also, if the PID parameters are not correctly chosen, control process input might be unstable, with or without oscillation; output diverges until it reaches a saturation or mechanical breakage.

For a system to operate properly, the output should be stable, and the process should

not oscillate in any condition of set point or disturbance. However, for some cases bounded oscillation condition as a marginal stability can be accepted. In today's control engineering world, PID is used over 95% of the control loops. Actually if there is control, there is PID, in analog or digital forms. In order to achieve optimum solutions, K_p, K_i and K_d gains are arranged according to the system characteristics. There are many tuning methods, but most common methods are the following:

- Trial & error tuning method
- Pole placement tuning method
- Ziegler-Nichols tuning method
- Cohen-Coon tuning method
- PID Tuning Software Methods (ex. MATLAB)

Among the classic controls used in the control of distributed generators, we can distinguish the Proportional-Integral control (PI). This command is characterized by simpler design and easier implementation. It is usually used by the implementation of the following transfer function :

$$C_{PI}(s) = K_p + \frac{K_i}{s} \tag{II.34}$$

In these systems, the efficiency of this controller can be improved by using compensation terms to compensate the cross coupling between currents and voltages. This controller ensures, in steady state, a perfect precision in the continuous (dq) frame. This zero static error consequently ensures less disturbed voltages and currents and a good active and reactive power flows with fewer oscillations.

However, despite these advantages, this type of controller is sensitive to parametric variations and uncertainties on the system parameters. Here, we preferred to use another control technique in the internal loop (level zero) which is more robust, this technique is the control by sliding mode that will be detailed later. While for the secondary control, a PI controller is sufficient and gives good performance.[20]

II.2.4 Sliding Mode Control

First introduced by Utkin in the late 1960s, the sliding mode control is a non-linear control technique applicable to both linear and nonlinear systems, it has received numerous attention regarding:

- Its relatively simple implementation.
- Its robustness with respect to disturbances and parameters variation.

The main principle of this technique is to steer the system to reach and stay on a given manifold in the phase space, called sliding surface, this surface being the sliding (hence the name sliding mode) or the switching surface, which is completely determined by the parameters and equations that describes that surface.

The advantage of having such a behavior is on one hand to reduce the order of the system in a way that it will be described by the sliding surface equations, and on the other hand, the sliding phase is insensitive to disturbances.

Historically speaking, the sliding mode control can be divided into two main types :

- First-order sliding mode control introduced by Utkin as mentioned before.
- Higher-order sliding mode control, which was generalized by Emelyanov et al. in the 1980s.

First Order Sliding Mode Control (FOSMC)

This type of sliding mode control consists of designing a discontinuous control law in a way that it makes the sliding surface attractive and invariant, at least locally.

Designing a sliding mode controller for a system should follow two steps[7] :

- The first step consists of defining a sliding surface in which sliding motion satisfies certain specifications, in other words, the the control objective is specified by that sliding surface.
- The second step is to design a control law that will drive the system onto that sliding surface, and by consequence, the desired behavior.

Let us consider this nonlinear single-input single-output following system:

$$\dot{x} = f(x,t) + g(x,t)u \tag{II.35}$$

Where $x \in \mathbb{R}^n$ is the state vector,$u \in \mathbb{R}$ is the input vector, and now we will define the new function $s(t,x)$ in a way that it fulfills the following:

$$\mathrm{S} = \{\mathrm{x} \in \mathrm{R}^n : \mathrm{s(t,x)} = 0\} \tag{II.36}$$

Represented as a manifold with the same dimension as the input u (one in this case), S is what is called a sliding surface, and the function $s(t,x)$ is the sliding function.

For the first order sliding mode control, it can be defined as a sliding mode controller in which the relative degree with respect to the control variable is equal to one (meaning that the control variable appears in the first derivative of the sliding function), meaning that:

$$\dot{\mathrm{s}} = h(x,u,t) \tag{II.37}$$

We can say that an ideal sliding on S exists if a restricted time t_s exists such that a control for equation (II.35) exists that satisfies $s(t,x) = 0$ for all $t \geq t_s$.

Notion of attraction :

For a sliding regime to exist, a sliding surface has to be locally attractive, which can be translated mathematically by the following:

$$\lim_{s\to 0^+} \frac{\partial s}{\partial x}(f+gu) < 0 \text{ and } \lim_{s\to 0^-} \frac{\partial s}{\partial x}(f+gu) > 0 \tag{II.38}$$

This condition assures that when the system is in proximity to the sliding surface, the speed vectors of the system's trajectories will always be pointing towards this surface, as we can see in the figure II.4:

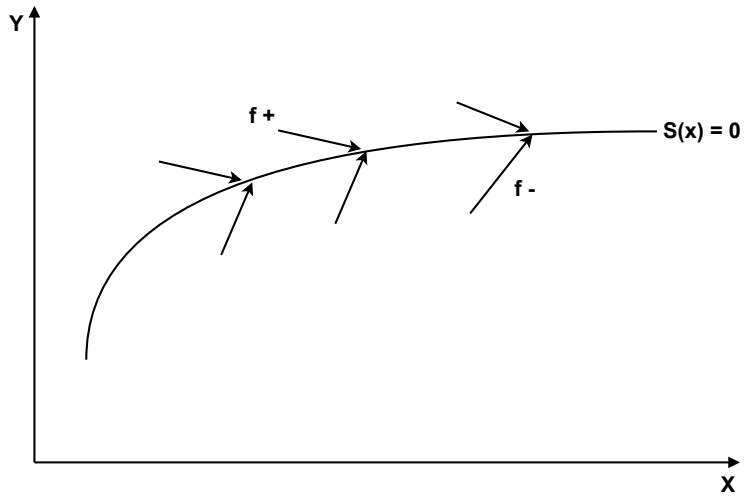

Figure II.4: Sliding surface attraction[6]

The condition (II.38), can be called an ideal sliding state (in which we have exactly $s(t,x) = 0$), if its reformulated to the following:

$$\dot{S}S < 0 \tag{II.39}$$

In addition, this is what is called the attraction condition.

The input u is formulated in a manner that the system's trajectories are steered towards that sliding surface and then made sure that it is maintained in its vicinity, a variable structured control law can be defined as the following :

$$u = \begin{cases} u^+(x) \text{ if } s(t,x) > 0 \\ u^-(x) \text{ if } s(t,x) < 0 \end{cases}, u^+ \neq u^- \tag{II.40}$$

When the system is restrained to the surface S, its behaviour can be determined by what is called the invariance condition.

$$\begin{aligned} &s = 0 \\ &\frac{\partial s}{\partial x}\left[f(x) + g(x)u_{eq}\right] = 0 \end{aligned} \tag{II.41}$$

With this being taken into consideration, an equivalent control as suggested by Utkin is given by the expression:

$$u_{eq}(x) = -\left[\frac{\partial s}{\partial x}g(x)\right]^{-1}\frac{\partial s}{\partial x}f(x) \tag{II.42}$$

This equivalent control is defined iff $\frac{\partial s}{\partial x}g(x) \neq 0$ on S. When realizing the variable structured control law, it can be divided into two parts, the first part is considered to be the equivalent control as shown by the equation (II.42), which assures the restraint of the system's dynamics in the sliding surface (what is called the sliding phase), and a discontinuous control, which assures the convergence in a finite time towards that surface (or what is called the reaching phase).
A classic example of this applied to the system (III.1) is as follows:

$$U = u_{eq} + u_{disc} \tag{II.43}$$

with

$$u_{disc} = -K\left[\frac{\partial s}{\partial x}g(x)\right]^{-1}\text{sign}(s) \tag{II.44}$$

Thus, the control law becomes :

$$u = u_{eq} - K\left[\frac{\partial s}{\partial x}g(x)\right]^{-1}\text{sign}(s) \tag{II.45}$$

Chattering phenomenon :

From a practical point of view, an ideal sliding regime does not exist because it has to imply that the control or the input could switch at an infinite frequency, meaning that our control law cannot actually check the $s = 0$ condition, this introduces a phenomenon called chattering (as shown in Figure (II.5)), which is characterized by strong oscillations around the sliding surface

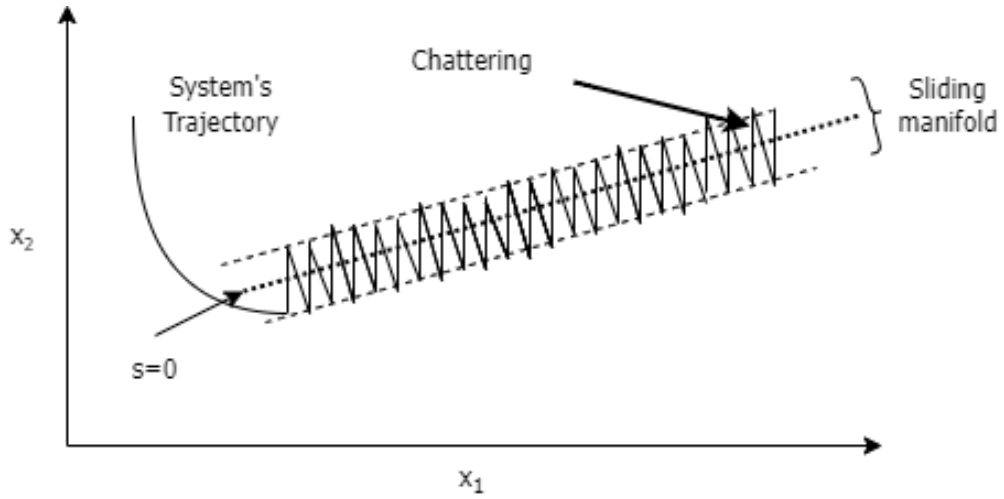

Figure II.5: Chattering phenomena[7]

This phenomenon is not favorable for any usage especially in power electronics, first because it can induce some significant power loss, it can also wear out the system's components faster than it should, and more importantly, if the system is not resilient to a degree it can lead to stability issues.

This is the salient reason that made researchers to introduce what is called Higher-order sliding mode control.

Higher Order Sliding Mode Control (HOSMC)

As we have mentioned before, the FOSMC is indeed a robust nonlinear control technique, but seeing its disadvantages (mainly the chattering phenomenon), researchers proposed a new way of sliding on the surface that makes the control smoother while keeping the advantages of sliding mode, namely its robustness, here we are speaking of Higher-Order Sliding Mode.

The name higher-order sliding mode control refers to the relative degree of the sliding function s. Opposed to the FOSMC, the objective is not only to cancel the sliding function itself, but all of the derivatives to the degree $r-1$ (r being the relative degree of the sliding function) meaning:

$$s = \dot{s} = \ddot{s} = \cdots = s^{r-1} = 0 \tag{II.46}$$

In our case, a Second-Order Sliding Mode Control (SOSMC) is applied, meaning that our sliding function should meet these requirements:

$$\begin{cases} s = \dot{s} = 0 \\ \frac{\partial s}{\partial u} = \frac{\partial \dot{s}}{\partial u} = 0 \\ \frac{\partial \ddot{s}}{\partial u} \neq 0 \end{cases} \tag{II.47}$$

The last two equations of (II.47) assure the relative degree being equal to two, the sliding manifold S can be described by the following figure:

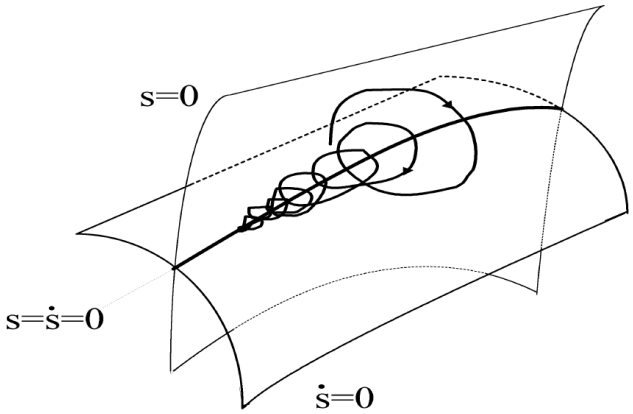

Figure II.6: Sliding manifold for the SOSMC[7]

There are a lot of algorithms that implement a control law for this type, but the one that we are interested in is the Twisting algorithm

Twisting algorithm[6] :

Let us consider the following sliding function :

$$s = x_n - x_{Ref} \tag{II.48}$$

With x_n being the state that the desired behavior is applied on and x_{Ref} the reference trajectory. In addition, let us consider this following representation of the second derivative of the sliding function s :

$$\ddot{s} = a(t,x) + b(t,x,u)U - \ddot{x_{Ref}} \tag{II.49}$$

The twisting algorithm states that the control law is of the form :

$$U = U_{eq} + U_{disc} \tag{II.50}$$

U_{eq} is calculated through cancelling $\ddot{s}$, meaning:

$$\ddot{s}|_{U_{eq}} = 0 \implies U_{eq} = \frac{-a(t,x) + \ddot{x_{Ref}}}{b(t,x,u)} \tag{II.51}$$

For U_{disc} two assumption have to be made :

$$\begin{cases} 0 < \Gamma_m < |b(t,x,u)| < \Gamma_M \\ |a(x,t)| \leq A \end{cases} \tag{II.52}$$

With that being established, we get :

$$U_{disc} = \begin{cases} -K_m \operatorname{sign}(s) & \text{if } s\dot{s} \leq 0 \\ -K_M \operatorname{sign}(s) & \text{if } s\dot{s} > 0 \end{cases} \tag{II.53}$$

With K_m and K_M satisfying these sufficient conditions:

$$\begin{cases} K_M > K_m \\ K_m > \frac{A}{\Gamma_m} \\ K_M > \frac{\Gamma_M K_m + 2A}{\Gamma_m} \end{cases} \tag{II.54}$$

II.3 Conclusion

In this chapter, we have discussed the modelling of our inverter, with first mentioning some presumptions that have to be made before starting to model, and then we have divided the modeling into two parts: an inverter's bridge and a LCL filter. After establishing a working model for the inverter, the control law implementation was split into two parts

- PID controller: in this part we have discussed the PID controllers as well as their wide usage in the industry, their advantages, and of course their disadvantages compared to other techniques like the next one.
- Sliding mode control : for this part, we have talked about the theory of sliding mode control, its advantages regarding to the PID control method, its disadvantages in some cases, and the way to implement and design a control law using sliding mode, especially the twisting algorithm which will then be used in the following chapter.

Chapter III

Microgrids Control

III.1 Introduction

In this part, and as we have already established in chapter 1 regarding the master/slave control or the droop control, our study subject will be based on the pairing of parallel inverters, for the first part our interest is going to be about establishing the first level of control shown in figure I.5 or voltage and current regulation. After that, the next two parts will be dedicated to trying to establish the primary control which is power sharing as well as the secondary control or the voltage frequency and amplitude restoration for the last control type.

III.2 Forming and following inverters control (Level Zero)

For the forming inverter, our interest is going to be about controlling the waveform of the capacitors' voltages, as for the following one, the second set of inductors' currents are the controlled states.

III.2.1 Forming Inverter Control

As we have mentioned before, the interest of control of a forming inverter is the capacitors' voltages, and going back to figure I.5 this control level is considered to be the level-zero control.

Although there is a plethora of control methods to achieve our goal, we will use the second order sliding mode control as we have mentioned in chapter two, where it has proven itself to be a robust control method with good disturbance rejection.

Going back to the second order sliding mode control design (Twisting algorithm), the choice of our sliding function will be made to satisfy the conditions mentioned in the equations (II.47).

Since we have two states to control, namely V_{C1} and V_{C2}, two sliding functions must be defined, s_1 and s_2. To drive the capacitor's voltages towards a desired trajectory, we have the

following sliding functions :

$$s_i = V_{Ci} - V_{CiRef} \quad ; \quad i = 1, 2. \tag{III.1}$$

With V_{Ci} being the $i-th$ capacitor's voltage and V_{CiRef} being the desired trajectory of V_{Ci}. by differentiating once and by coming back the system's dynamics (equation (II.26)), it yields:

$$\dot{S}_i = \dot{V_{Ci}} - \dot{V_{CiRef}} = \frac{1}{C} I_{Li} - I_{Oi} - \dot{V_{CiRef}} \quad ; \quad i = 1, 2. \tag{III.2}$$

And by differentiating equation (III.2) we get

$$\ddot{S}_i = \frac{1}{C} \dot{I_{Li}} - \dot{I_{Oi}} - \ddot{V_{CiRef}} \quad ; \quad i = 1, 2.$$

$$\ddot{S}_i = -\frac{1}{LC} V_{Ci} + \frac{V_{DC}}{LC} U_i - \frac{V_{DC}}{2LC} - \frac{1}{C} \dot{I_{Oi}} - \ddot{V_{CiRef}} \quad ; \quad i = 1, 2. \tag{III.3}$$

According to the Twisting algorithm as described in the second chapter (equation (II.50)), our control law can be described as :

$$U = U_{eq} + U_{disc} \tag{III.4}$$

When it comes to equivalent control U_{eq}, it can be described as the following :

$$S|_{U_{ieq}} = 0 \quad \Longrightarrow \; -\frac{1}{LC} + \frac{V_{DC}}{LC} U_{ieq} - \frac{V_{DC}}{2LC} - \frac{1}{C} \dot{I_{Oi}} - \ddot{V_{CiRef}} = 0 \quad ; \quad i = 1, 2.$$

$$U_{ieq} = \frac{LC}{V_{DC}} \left[\frac{1}{LC} V_{Ci} + \frac{1}{C} \dot{I_{Oi}} + \ddot{V_{CiRef}} \right] \quad ; \quad i = 1, 2. \tag{III.5}$$

As for U_{disc}, if we could describe $\ddot{S}$ as equation (II.49), we would get :

$$\begin{cases} a_i(t, x) = -\frac{1}{LC} V_{Ci} - \frac{1}{C} \dot{I_{Oi}} \\ b_i(t, x, u) = \frac{V_{DC}}{LC} \end{cases} \quad ; \quad i = 1, 2. \tag{III.6}$$

After defining Γ_m, Γ_M and A as mentioned in equation (II.52), U_{disc} can be written as :

$$U_{idisc} = \begin{cases} -K_{mi} sign(s) & s\dot{s} \leq 0 \\ -K_{Mi} sign(s) & s\dot{s} > 0 \end{cases} \quad ; \quad i = 1, 2. \tag{III.7}$$

with K_{mi} and K_{Mi} satisfying the condition of (II.54). The final expression of the control law :

$$Ui = U_{ieq} + U_{idisc} = \frac{LC}{V_{DC}}\left[\frac{1}{LC}V_{Ci} + \frac{1}{C}\dot{I}_{Oi} + \ddot{V}_{CiRef}\right] + \begin{cases} -K_{mi}sign(s) & s\dot{s} \leq 0 \\ -K_{Mi}sign(s) & s\dot{s} > 0 \end{cases} \quad ; \quad i = 1, 2. \tag{III.8}$$

To apply this control on inverters or more generally on any power electronics application, the control method is mostly based on Pulse Width Modulation or PWM, for this purposes, the controller generates the proper duty cycles that are compared with a triangular waveform in which the frequency is equal to the desired switching frequency of the switches. In the case of inverters, the desired wave-forms of voltage or current are sinusoidal, the generated duty cycles are sinusoidal as well, but centered in 0.5 as it can be seen in the Figure III.1 :

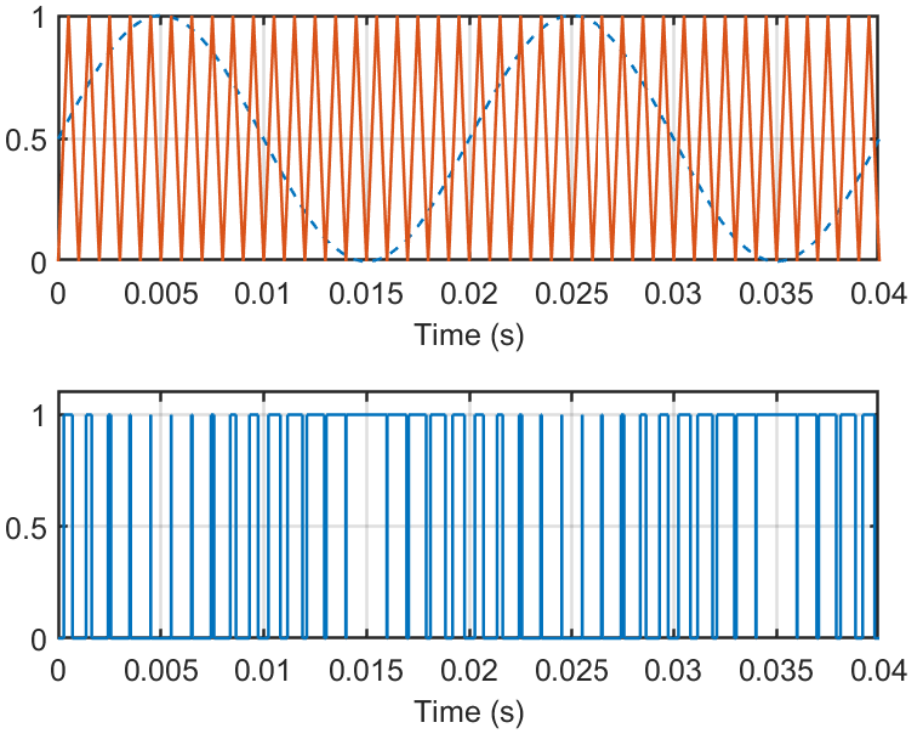

Figure III.1: Pulse Width Modulation applied to an inverter

For this part, we carried out a simulation containing an inverter with the following parameters :

DC voltage supply V_{DC}	700 V
First set of inductors	L= 8mH
Second set of inductors	$L^{'}$ = 6mH
Capacitors	C = 50µF

Table III.1: Forming Inverter Parameters[1]

As well as the controls mentioned by (III.8), the generated duty cycles are modulated using a triangular signal with a frequency of 10kHz.

To have this type of modulation to operate properly, the generated duty cycles by the controller (in this case the control) must remain within the range $[0, 1]$, for this constraint to be met, the sliding mode gains are set to $K_m = 0.01$ $K_M = 0.1$.

The switching devices chosen in the following tests are IGBTs, they should suffice for a switching frequency of 10kHz. The proposed control scheme can be shown in figure III.2 :

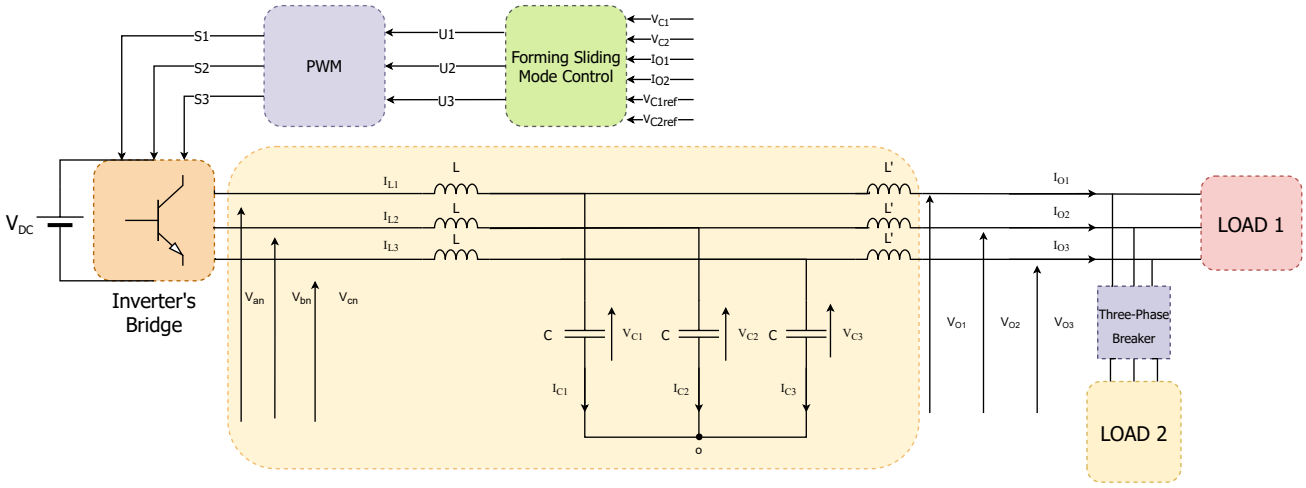

Figure III.2: Forming inverter control scheme

For the testing, a reference signal of $V_{Ref1} = 220\sqrt{2}\sin(2\pi ft)$, $V_{Ref2} = 220\sqrt{2}\sin(2\pi ft - \frac{2\pi}{3})$ with the frequency f being set to 50Hz is applied to both V_{C1} and V_{C2} respectively, the simulation time is set to 0.5s, the first load power demands 5kW and 1kVAR of active and reactive powers, at 0.25s, the three-phase breaker closes and the second load power demands are 3kW and 4kVAR. The results are as follows :

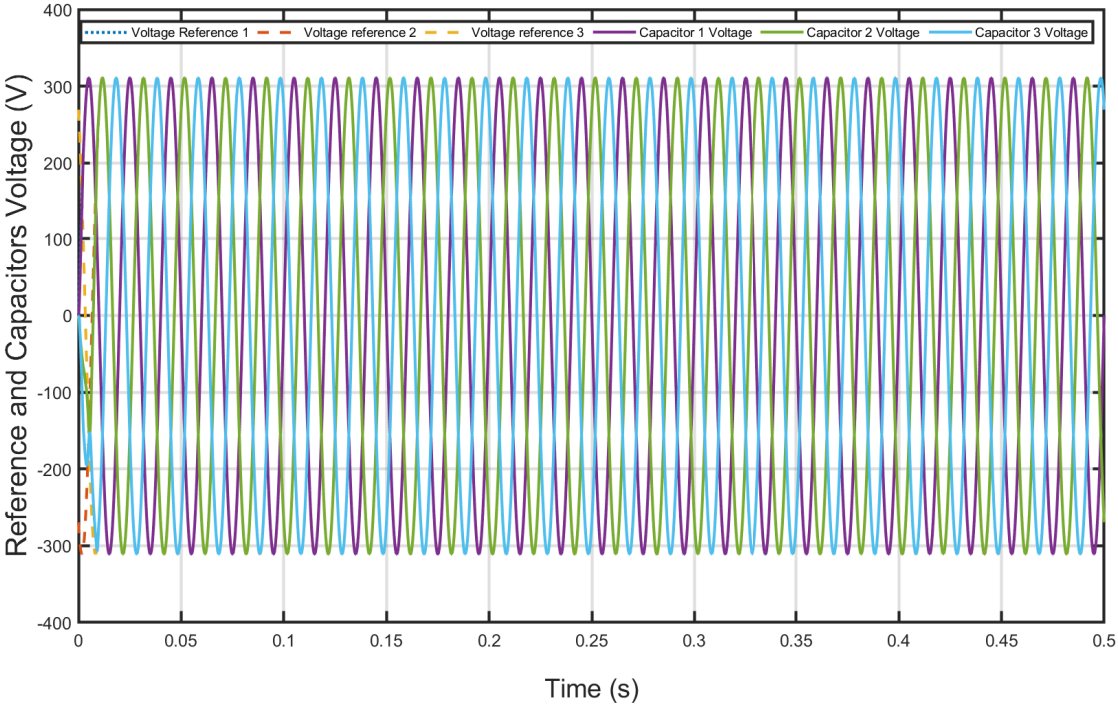

Figure III.3: Reference and Capacitors voltages

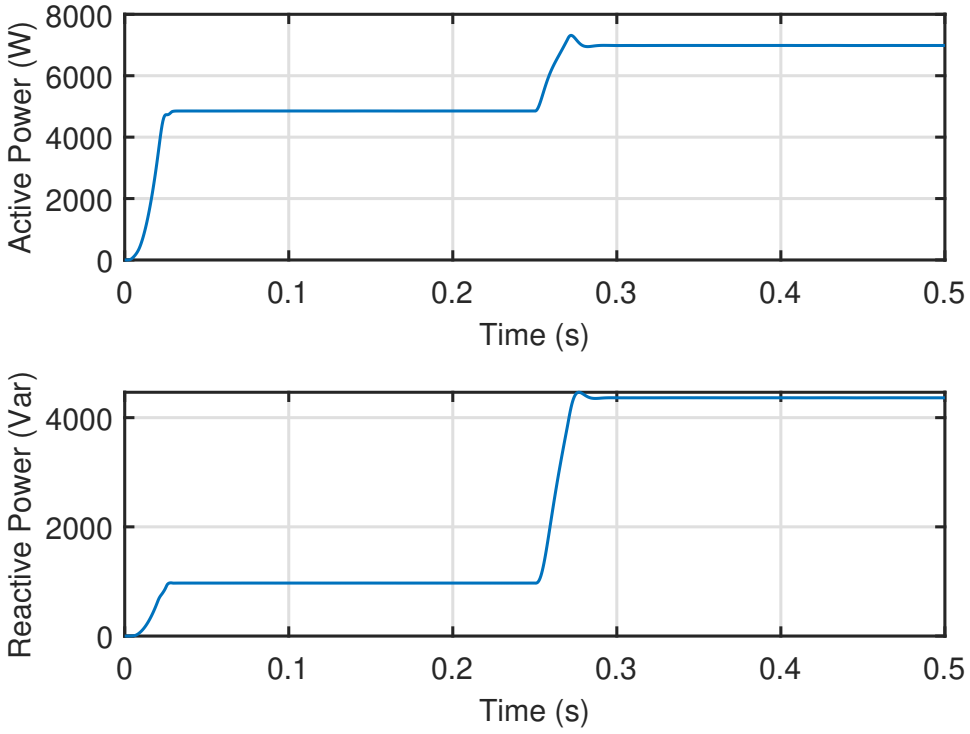

Figure III.4: Active and Reactive Power

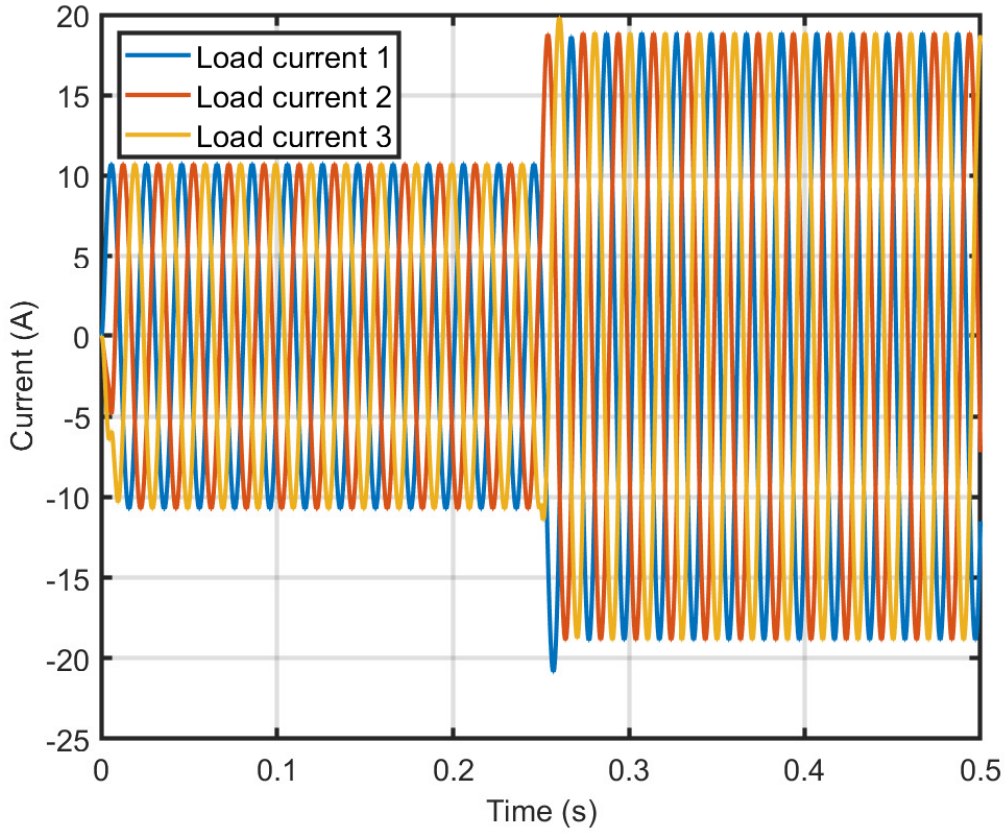

Figure III.5: Output Current

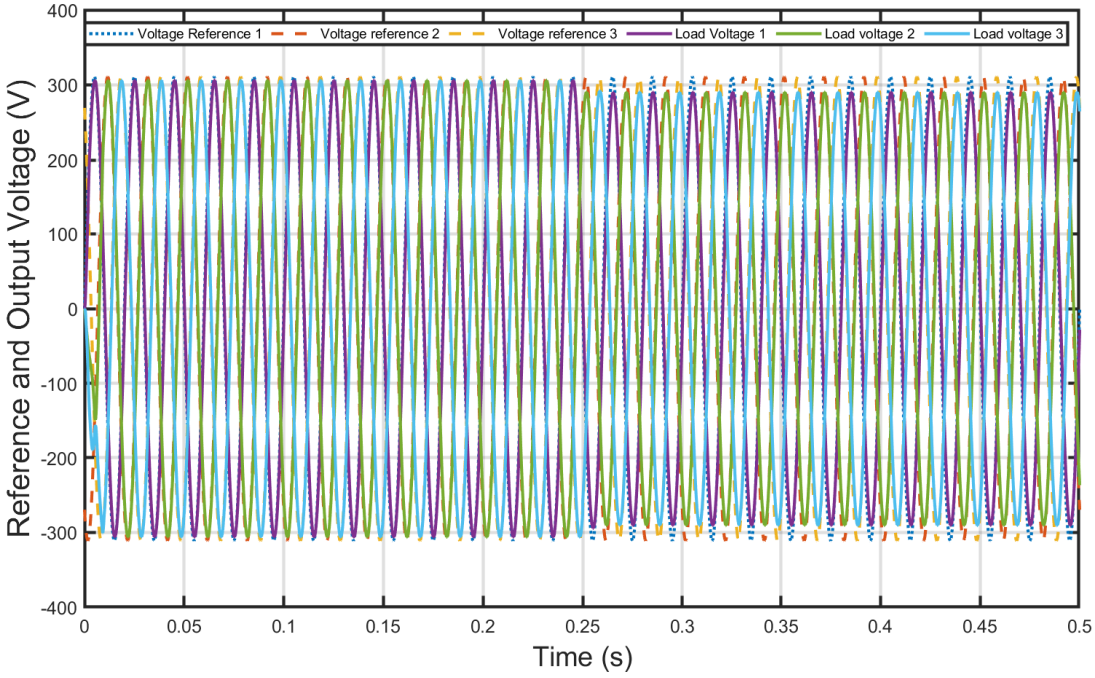

Figure III.6: Reference and Output Voltages

As we can see from figures III.4 and III.6, the power demands are not actually met as well as the output voltages are not the same as the reference voltages, the explanation is that the reference signal is applied to the capacitors and from figure III.3 they are overlapping, but between the output voltages and the capacitor voltages there are the second set of inductors voltages that were not taken into consideration, to construct the new reference signal we have:

$$V_{L'i} = V_{Ci} - V_{Oi} \quad ; \quad i = 1, 2 \tag{III.9}$$

The reference signal should be of the following form :

$$\begin{cases} V_{Ref1} = 220\sqrt{2}\sin(2\pi ft) + V_{L'1} \\ V_{Ref2} = 220\sqrt{2}\sin(2\pi ft - \frac{2\pi}{3})) + V_{L'2} \end{cases} \tag{III.10}$$

After doing so, the new results are :

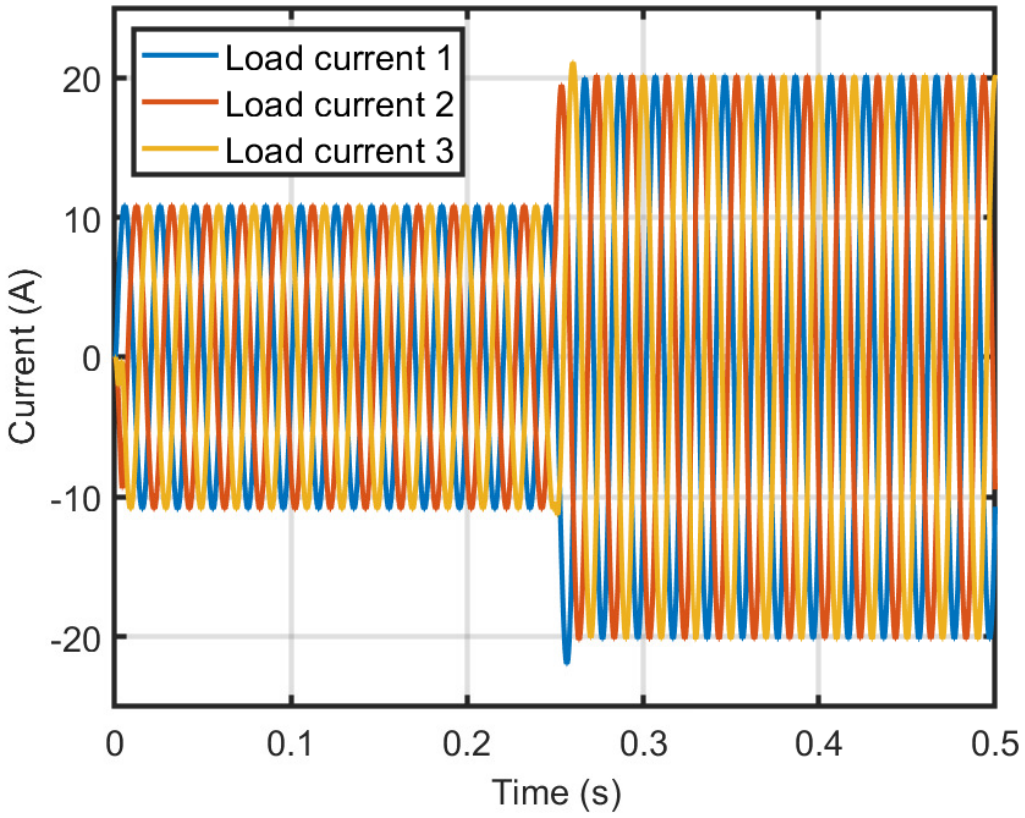

Figure III.7: Output Current after reference correction

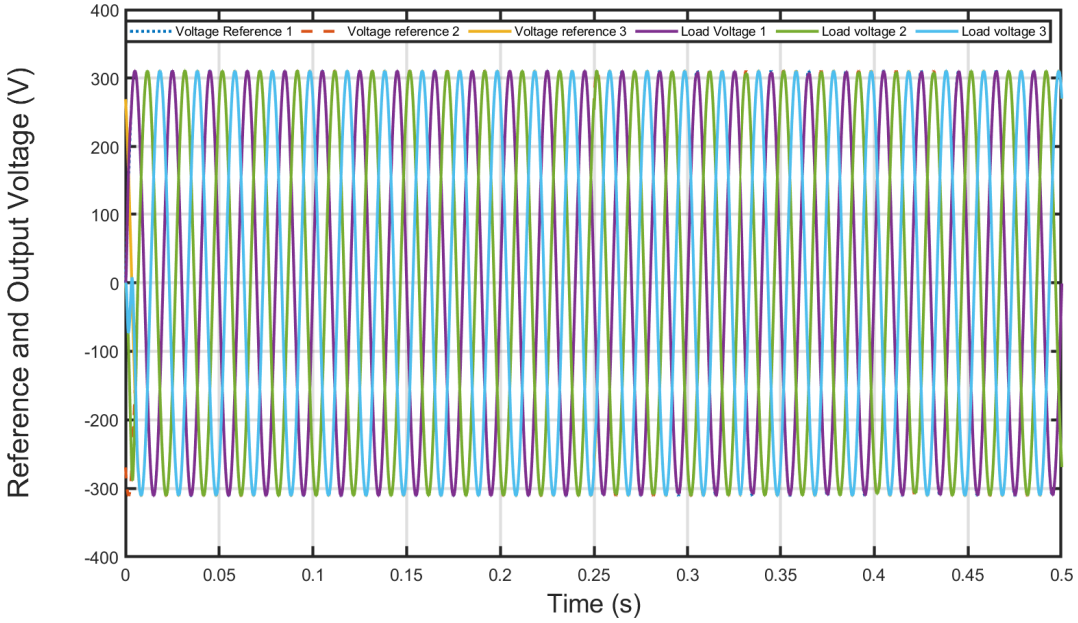

Figure III.8: Reference and Output Voltages after reference correction

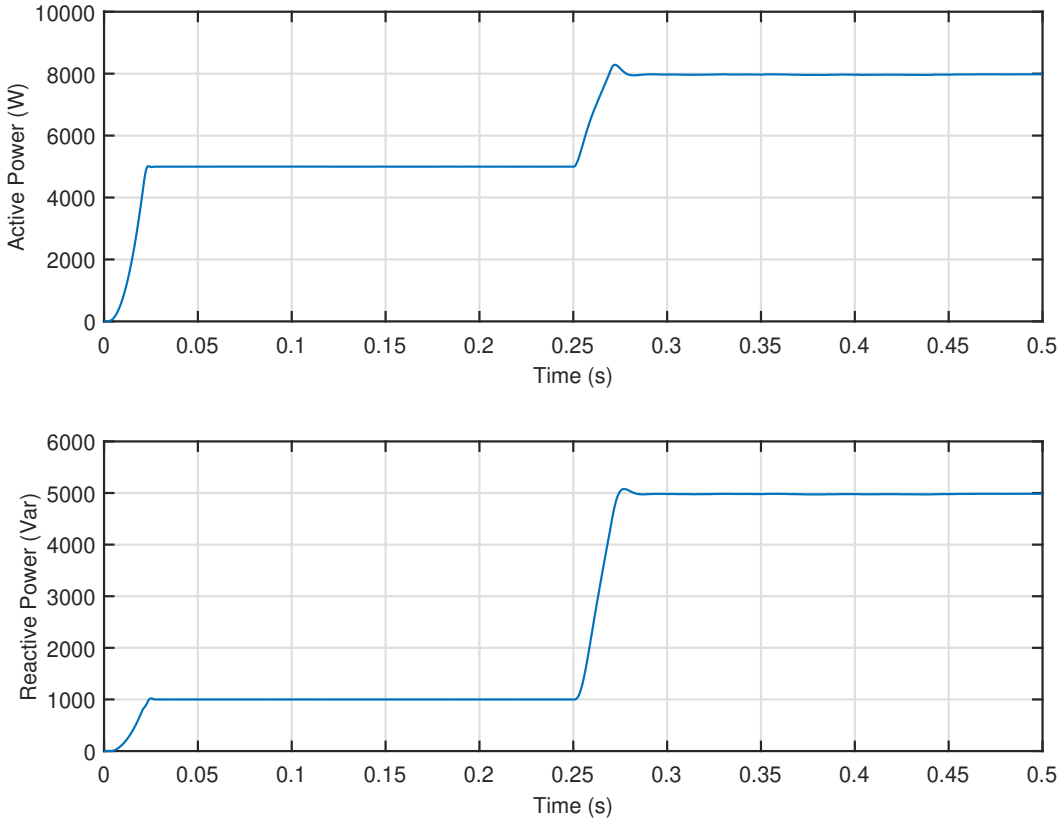

Figure III.9: Active and Reactive Power after reference correction

As we can see, both active and reactive power demands are met with good reference tracking for the output voltages.

III.2.2 Following inverter

For the following inverter, our control interest is driven towards the output currents or more precisely the current of the second set of inductors, the choice of a sliding function in this differs from the forming inverter because the control expression is not explicitly shown in the second derivative of the two states that represent the output currents I_{O1} and I_{O2} meaning that :

$$\frac{\partial \ddot{S}_i}{\partial u} = 0 \quad ; \quad i = 1, 2. \tag{III.11}$$

To overcome this, a sliding function choice made by JJE. Slotine [21] consists of calculating the relative degree n of the sliding function (in our case it is 2) and then choose a function of $(n-1)th$ order, our new sliding function is written as follows :

$$S_i = \dot{e_i} - \lambda e_i. \tag{III.12}$$

With e being the error between the output current and its reference signal and λ is a gain that helps with the convergence speed of the solution, by following the choice of equation (III.12) we get:

$$S_i = (\dot{I_{Oi}} - \dot{I_{OiRef}}) - \lambda(I_{Oi} - I_{OiRef}) \quad ; \quad i = 1, 2 \tag{III.13}$$

$$S_i = \frac{1}{L'}(V_{Ci} - VOi) + \lambda I_{Oi} - (\dot{I_{ORef}} + \lambda I_{Oref}) \quad ; \quad i = 1, 2 \tag{III.14}$$

By differentiating (III.14) we get

$$\dot{S}_i = \frac{1}{L'}\dot{V_{Ci}} - \frac{1}{L'}\dot{V_{Oi}} + \lambda\dot{I_{Oi}} - (\ddot{I_{ORef}}) + \lambda\dot{I_{Oref}}) \quad ; \quad i = 1, 2 \tag{III.15}$$

$$\dot{S}_i = \frac{1}{L'C}(I_{Li} - I_{Oi}) + \frac{\lambda}{L'}(V_{Ci} - V_{Oi}) - (\frac{1}{L'}\dot{V_{Oi}} + \ddot{I_{ORef}} + \lambda\dot{I_{Oref}}) \quad ; \quad i = 1, 2 \tag{III.16}$$

As for the second derivative

$$\ddot{S}_i = \frac{1}{L'C}\dot{I_{Li}} - \frac{1}{L'C}\dot{I_{Oi}} + \frac{\lambda}{L'}\dot{V_{Ci}} - (\frac{1}{L'}\dot{V_{Oi}} + \frac{1}{L'}\ddot{V_{Oi}} + I^{(3)}_{ORef} + \lambda\ddot{I_{ORef}}) \quad ; \quad i = 1, 2 \tag{III.17}$$

If we take $B = (\frac{1}{L'}\dot{V_{Oi}} + \frac{1}{L'}\ddot{V_{Oi}} + I^{(3)}_{ORef} + \lambda\ddot{I_{ORef}})$, we get :

$$\ddot{S}_i = \frac{1}{L'CL}(-V_{Ci} + V_{DC}U_i - \frac{V_{DC}}{2}) - \frac{1}{CL'^2}(V_{Ci} - V_{Oi}) + \frac{\lambda}{L'C}(I_{Li} - I_{Oi}) - B \quad ; \quad i = 1, 2 \tag{III.18}$$

Finally, the second derivative of the sliding function is of the form :

$$\ddot{S}_i = \frac{V_{DC}}{L'CL}U_i - \frac{1}{L'CL}(V_{Ci} + \frac{V_{DC}}{2}) - \frac{1}{CL'^2}V_{Ci} + \frac{\lambda}{L'C}(I_{Li} - I_{Oi}) + \frac{1}{CL'^2}V_{Oi} - B \quad ; \quad i = 1, 2 \tag{III.19}$$

Going back to equation (III.4), and by applying the twisting algorithm we get :

$$S|_{U_{ieq}} = 0 \quad \Longrightarrow \frac{V_{DC}}{L'CL}U_{ieq} - \frac{1}{L'CL}(V_{Ci} + \frac{V_{DC}}{2}) - \frac{1}{CL'^2}V_{Ci} + \frac{\lambda}{L'C}(I_{Li} - I_{Oi}) + \frac{1}{CL'^2}V_{Oi} - B = 0 \quad ; \quad i = 1, 2. \tag{III.20}$$

$$U_{ieq} = \frac{L'CL}{V_{DC}}\left[\frac{1}{L'CL}(V_{Ci} + \frac{V_{DC}}{2}) + \frac{1}{CL'^2}V_{Ci} - \frac{\lambda}{L'C}(I_{Li} - I_{Oi}) - \frac{1}{CL'^2}V_{Oi} + B\right] \quad ; \quad i = 1, 2. \tag{III.21}$$

As for U_{disc} :

$$\begin{cases} a_i(t,x) = -\frac{1}{L'CL}(V_{Ci} + \frac{V_{DC}}{2}) - \frac{1}{CL'^2}V_{Ci} + \frac{\lambda}{L'C}(I_{Li} - I_{Oi}) + \frac{1}{CL'^2}V_{Oi} \\ -\frac{1}{L'CL}(\frac{V_{DC}}{2}) + \frac{1}{CL'^2}V_{Oi} + \frac{1}{L'}\dot{V_{Oi}} + \frac{1}{L'}\ddot{V_{Oi}} \quad ; \quad i = 1, 2. \\ b_i(t,x,u) = \frac{V_{DC}}{L'CL} \end{cases} \tag{III.22}$$

After choosing appropriate values of K_{mi} and K_{Mi} according to the algorithm, the control law can be described by the following :

$$Ui = U_{ieq} + U_{idisc} = \frac{L'CL}{V_{DC}}\left[\frac{1}{L'CL}(V_{Ci} + \frac{V_{DC}}{2}) + \frac{1}{CL'^2}V_{Ci} - \frac{\lambda}{L'C}(I_{Li} - I_{Oi}) - \frac{1}{CL'^2}V_{Oi} + B\right] + \begin{cases} -K_{mi}sign(s) & s\dot{s} \leq 0 \\ -K_{Mi}sign(s) & s\dot{s} > 0 \end{cases} \quad ; \quad i = 1, 2. \tag{III.23}$$

Because a following inverter is usually paired with a forming inverter or tied to a three phase voltage source so that its output voltage can be imposed by it, we can simulate it by using a 1kΩ load and a reference of :

$$\begin{cases} I_{ORef1} = 20\sin(2\pi ft) \\ I_{ORef2} = 20\sin(2\pi ft - \frac{2\pi}{3})) \end{cases} \tag{III.24}$$

This reference is chosen for a 1kΩ load under an RMS voltage of $220\sqrt{2}$, this is why for

testing purposes we used an ideal three-phase generator that can supply that voltage as shown in figure III.10 :

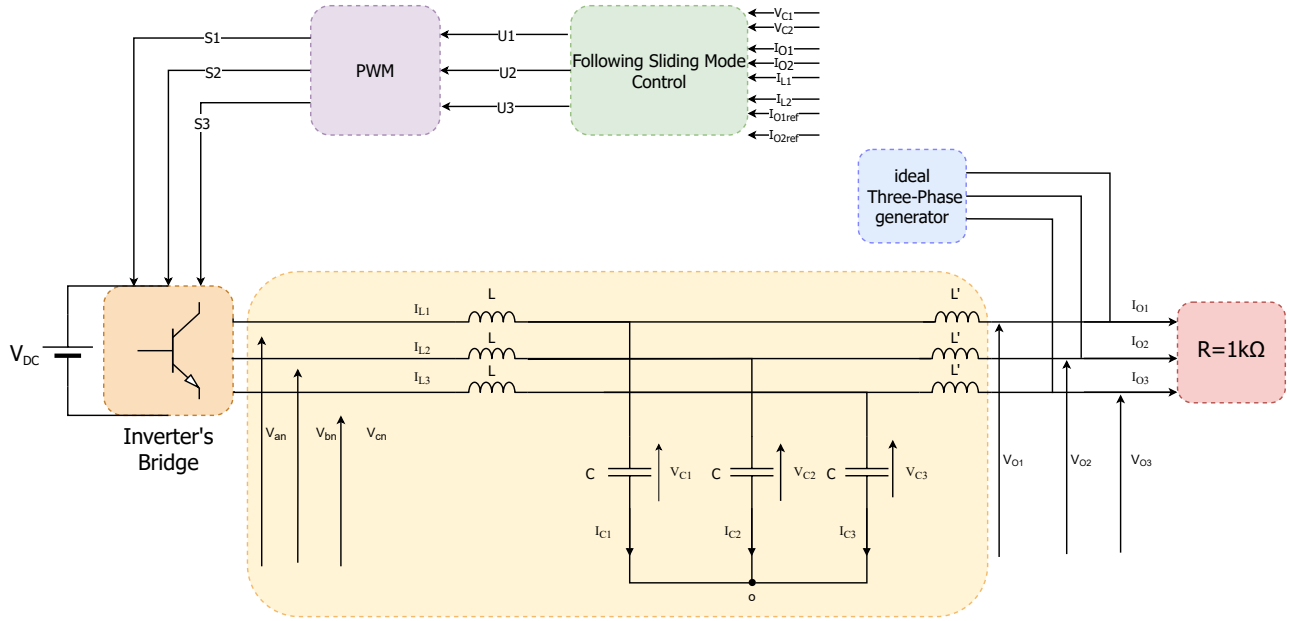

Figure III.10: Proposed control scheme for a single following inverter

The sliding mode gains K_{mi} and K_{Mi} are both set to 0.05 and 0.5 respectively, λ is set to 10^4 :

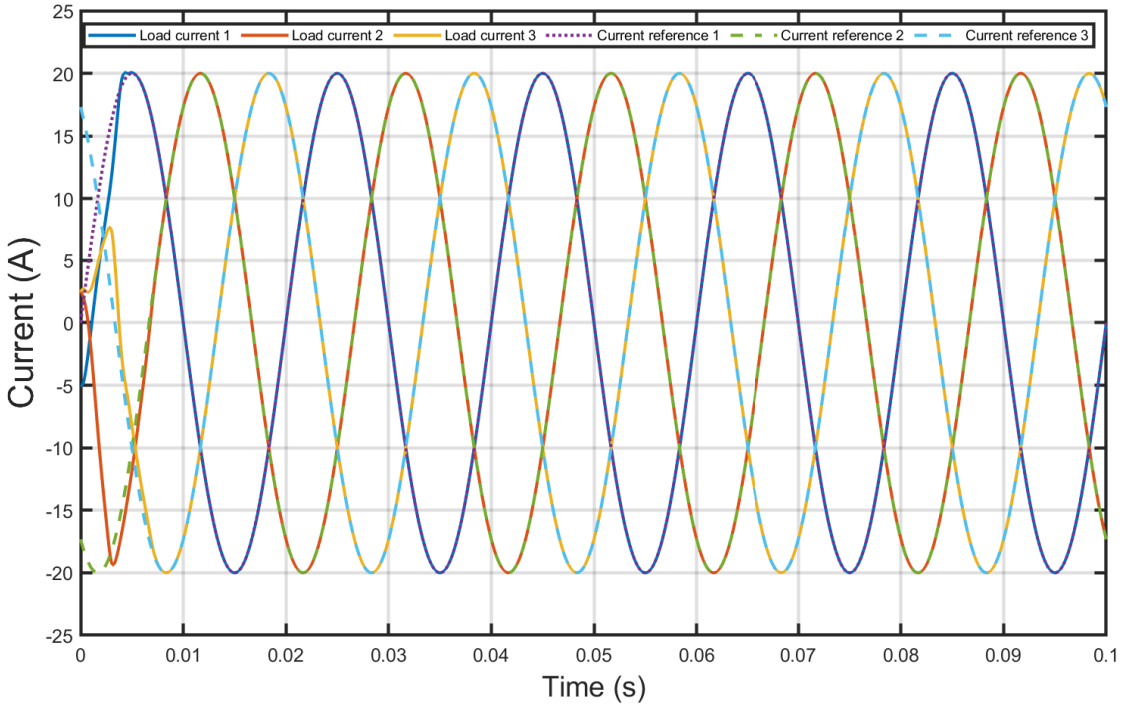

Figure III.11: Reference and output current of a single following inverter

As we can see in the figure III.11, the output current quickly catches up with the reference signal (in less than 10ms). After being done with the first level of microgrids control, in the next two sections we are going to be dealing with both the primary control and the secondary control.

III.3 Centralized control

For a standalone microgrid with centralized control, we will use forming-following setup and we need three levels of control.

Regarding to the zero level control, we will control the waveform of the capacitors' voltages of the first inverter (forming) and the currents of the second set of inductors of the second inverter (following). For this purpose we have used the second-order sliding mode control, namely Twisting algorithm. The calculation steps and results of the control (for each inverter separately) are already illustrated in section III.2.

For centralized primary control. We will use in this work the Master/Slave method with central controller because it is relatively simple to implement compared to other centralized techniques. This technique is already explained in section I.10.1.

At last. This technique (Master/Slave) does not require a secondary control because it does not generate variations on the frequency and the amplitude of the voltage. These last two are already provided by the zero level control.

III.3.1 Simulation results

All simulations were performed in MATLAB/Simulink (R2021b). the table III.2 represents the parameters used for this part of simulation.

Simulation solver	ode8 (Dormand-Prince)
DC voltage supply V_{DC}	700 V
First set of inductors	L= 8mH
Second set of inductors	$L^{'} = 6$mH
Capacitors	C = 50µF

Table III.2: Master/Slave Simulation parametres[1]

The simulation scheme is illustrated in a block diagram as shown in Figure III.12

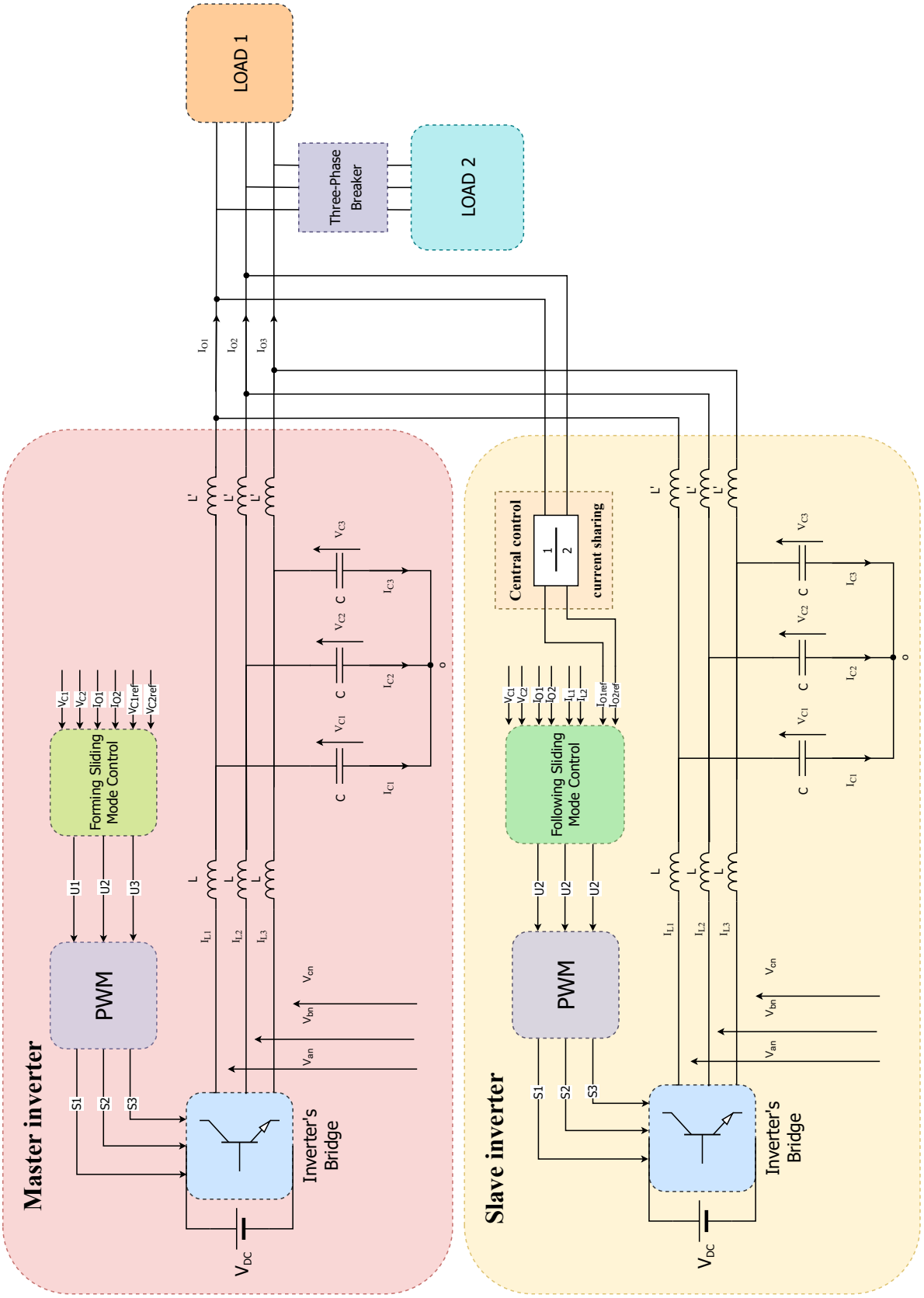

Figure III.12: Block diagram of simulation scheme

We can see in the figures below, the simulation results for two loads, the first load starts at the beginning of the simulation, the second one is introduced at $t = 0.08$s, the table III.3 represents the parameters of each load :

Load 1 Phase to phase voltage	$220\sqrt{3}$V
Load 2 Phase to phase voltage	$220\sqrt{3}$V
Load 1 Active power demand	5kW
Load 2 Active power demand	4kW
Load 1 Reactive power demand	$2kVAR$
Load 2 Reactive power demand	$5kVAR$

Table III.3: First and second load specifications

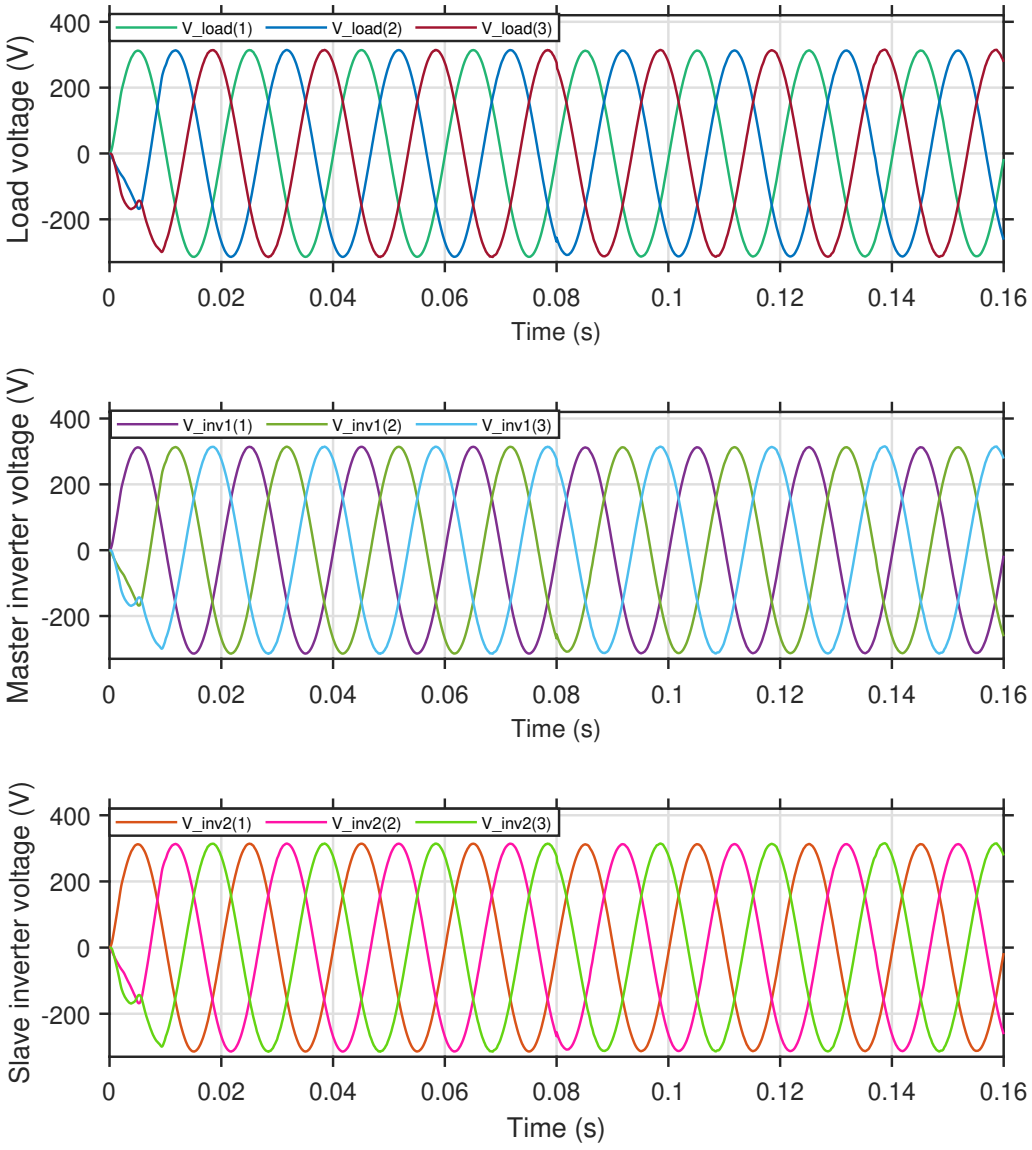

Figure III.13: Voltage of the load and both inverters (master & slave)

Figure III.13 presents the voltage of the loads and the voltage of the first inverter (Master) as well as the second inverter (Slave). From this figure we can notice that the voltage control is robust when we connected a second load at time $t = 0.08s$.

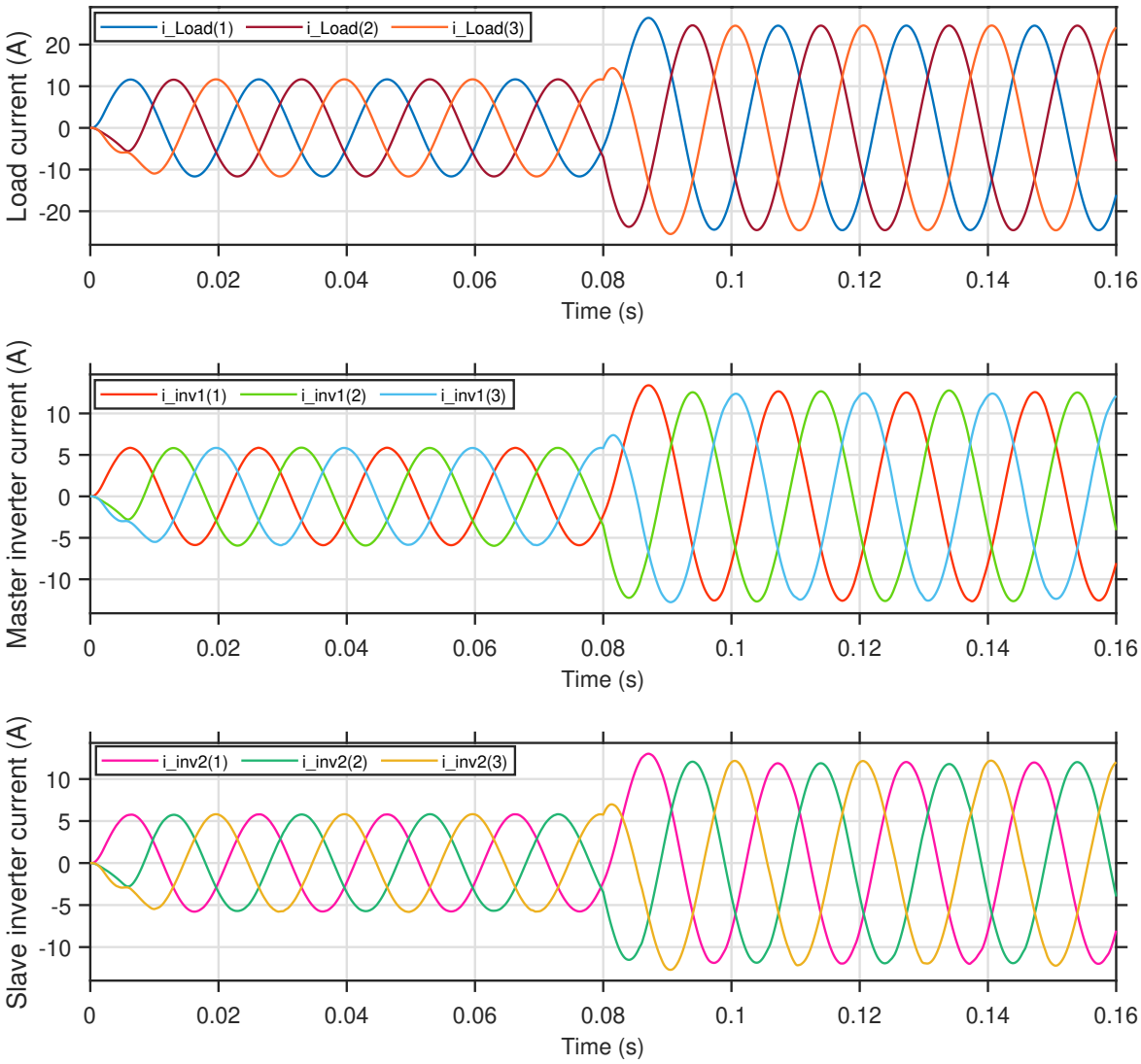

Figure III.14: Current of the load and both inverters (master & slave)

Figure III.14 shows that the Master/Slave technique divides almost equally the current absorbed by the load between the inverters available in the microgrid.

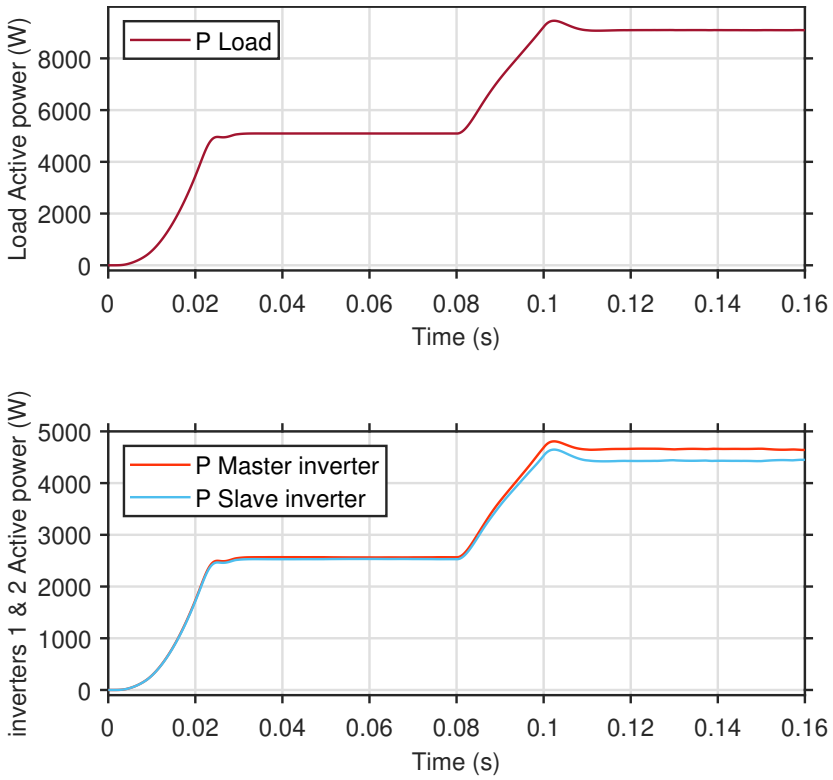

Figure III.15: Active power of the load and both inverters (master & slave)

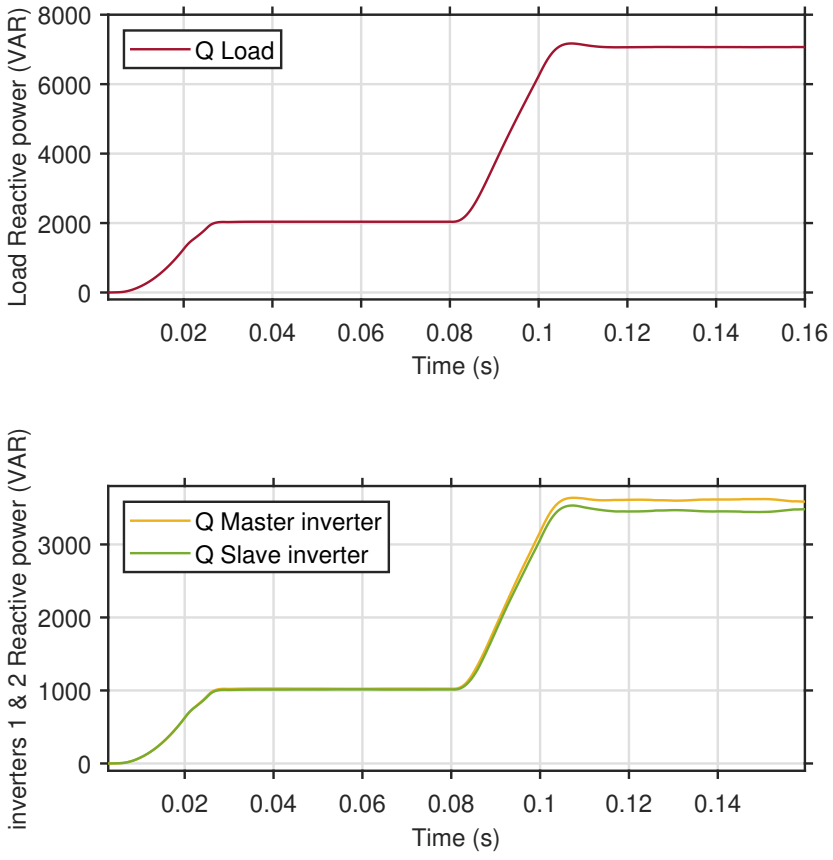

Figure III.16: Reactive power of the load and both inverters (master & slave)

Figures III.15 and III.16 allow us to observe the equally shared power between the two inverters thanks to this technique. In summary, master/slave control can achieve excellent power sharing performance plus its ease of implementation advantage [22]. But despite this, communication-based approaches, especially Master/slave technique has some drawbacks including: the need for high-bandwidth communication channels, which can be impractical and costly in microgrids with long connection distances between inverters, a relatively fast slave unit controller and the presence of a unit acting as a central control or a master which creates a single point of failure. If the master unit fails, the whole system will. [23]

A simple non-communication-based power sharing strategy can be realized in the sense of frequency and voltage droop method. The advantage of the droop method is that it does not require communication signals amongst units in parallel, thereby enhancing the system reliability.

III.4 Decentralized Control

III.4.1 Droop control

For this part, we will be applying the droop control technique on a parallel setup of Forming/Forming inverters. In a line that is predominantly inductive, the conventional P/f-Q/V droop technique can be applied which allows distributed generation systems to emulate the behavior of a synchronous generator as we have seen in Figure I.8.

Figure III.17 explains how droop control can be applied to obtain both voltage and frequency references :

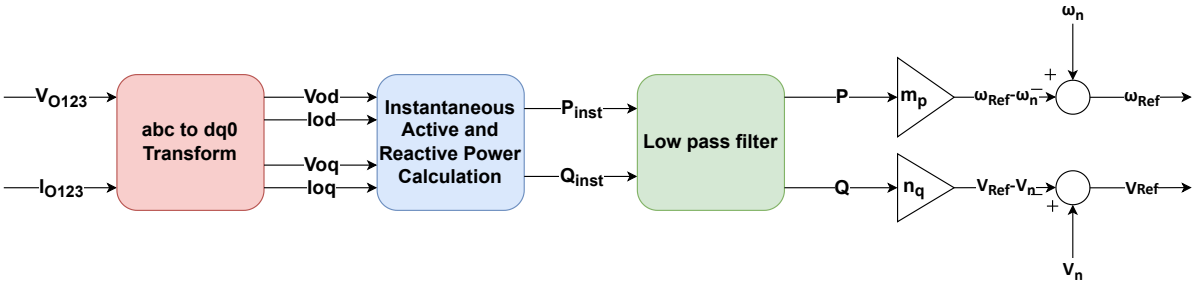

Figure III.17: Droop control scheme[5]

As we can see from figure III.17, we first have to calculate the instantaneous active and reactive power using the following equation :

$$\begin{bmatrix} P_{inst} \\ Q_{inst} \end{bmatrix} = \frac{3}{2} \begin{bmatrix} V_{od} & V_{oq} \\ V_{oq} & -V_{od} \end{bmatrix} \begin{bmatrix} I_{od} \\ I_{oq} \end{bmatrix} \tag{III.25}$$

Then, these power are ran through a low pass filter with a cutoff frequency of ω_c whose

output calculates the fundamental components P and Q. Both the references of the voltage's amplitude and frequency are calculated following these equations

$$\omega_{Ref} = \omega_n - m_p(P - P^*) \tag{III.26}$$

$$V_{Ref} = V_n - n_q(Q - Q^*) \tag{III.27}$$

The droop coefficients m_p and n_q are calculated by the equation mentioned in the first chapter, a reminder of those equation :

$$\begin{aligned} m_p &= \frac{\omega_{max} - \omega_{min}}{P_{max}} \\ n_q &= \frac{V_{max} - V_{min}}{Q_{max}} \end{aligned} \tag{III.28}$$

Where $\omega_{max} - \omega_{min}$ and $V_{max} - V_{min}$ are chosen accordingly to their according allowed norms, P_{max} and Q_{max} are the maximum active and reactive power respectively.
Now to apply this method on a parallel setup of two forming inverters, the droop coefficients chosen are set to $m_p = 10^{-5}$ and $n_q = 3.111 \cdot 10^{-5}$, these values represent a frequency deviation of $\pm 1\%$ and a voltage deviation of $\pm 5\%$ and an active and reactive power rating of 10^5W and 10^4 VAR.

There are two loads that are used to test the system, the first one is rated at 5kW and 2kVAR, the second one comes up at the half of the simulation time with 4kW and 5kVAR, making the total active and reactive powers at the end of the simulation ratings at 9kW and 7 kVAR, it has to be noted that for the two loads, to properly consume those powers, their phase-to-phase voltage rating is set to $V = 220\sqrt{3}$V, so the nominal voltage and nominal frequency in radiant of the droop control are set to 220 V RMS and $2\pi f_n$ with f_n being set to 50Hz, the cutoff frequency of the low-pass filter is set to $10\pi \frac{\text{rad}}{\text{s}}$.

The reference signal applied to both inverters are the reference voltage amplitude and frequency calculated from the droop control as shown in figure III.17 as well as taking into consideration the voltage of the second set of inductors for each inverter as we have already mentioned in the forming inverter part of this chapter (equation (III.10) specifically), the simulation results are as follows:

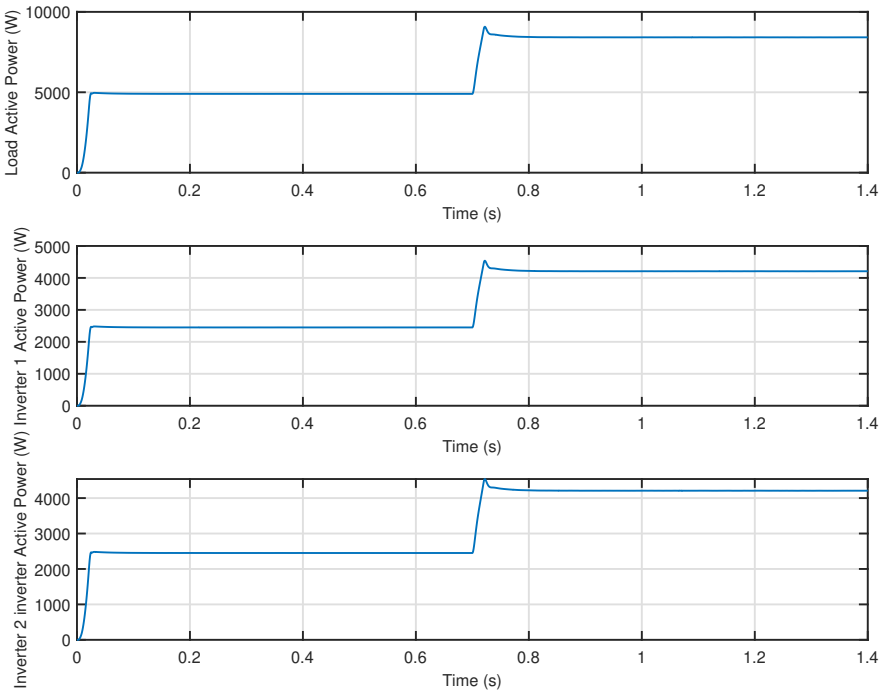

Figure III.18: Active power of the load and both inverters

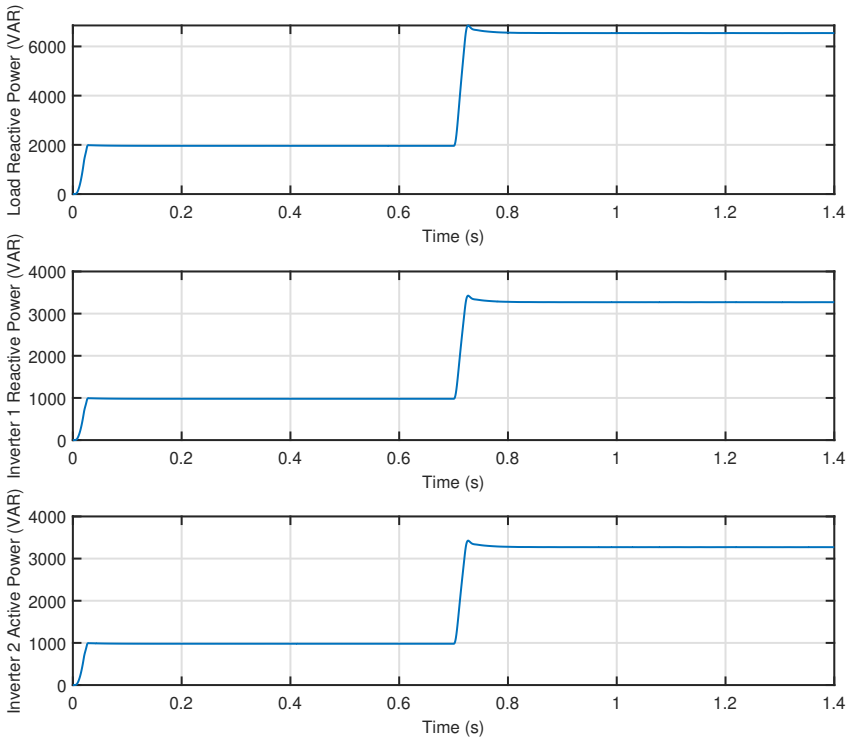

Figure III.19: Reactive power of the load and both inverters

As we can see from both figures III.18 and III.19, both active and reactive power demands are not met, in fact, at the end of the simulation both inverters should be giving out 4.5kW and 3.5kVAR but instead, they are giving less than expected. The explanation of that can be shown in the next two figures :

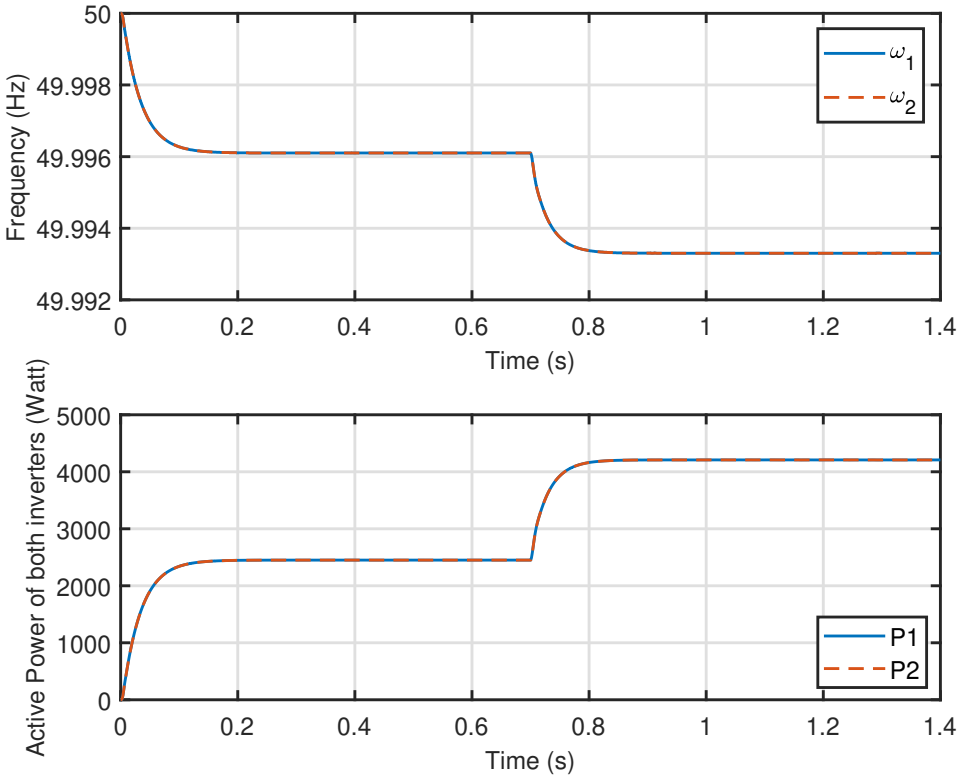

Figure III.20: Active power and frequency of both inverters

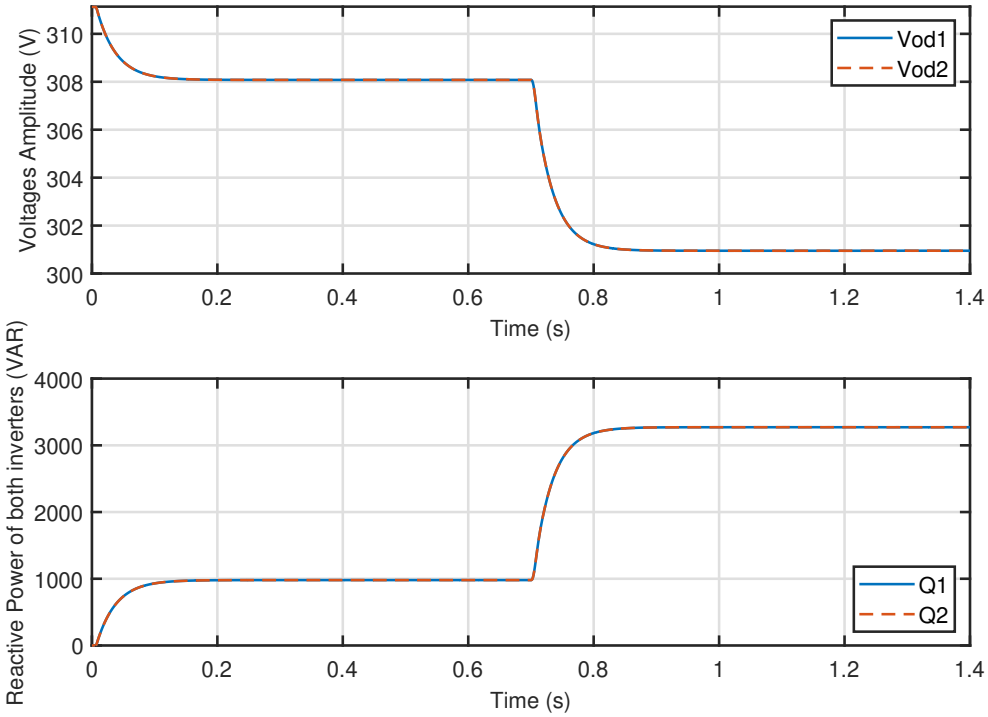

Figure III.21: Reactive power and voltage amplitude of both inverters

As we can see from figures III.20 and III.21 both frequency and amplitude of the voltage fall due to the droop control, where the load's rated phase-to-phase voltage and frequency are set to $220\sqrt{(3)}$ V and 50Hz, respectively. to solve this issue, a voltage and frequency restoration control loop must be applied.

III.4.2 Voltage amplitude and frequency restoration

In this part, and to restore the voltage's amplitude and frequency to their nominal values, the droop equations as described in III.26 and III.27 can be reformulated into the following :

$$\omega_{Ref} = \omega_n - m_p P + \Delta\omega \tag{III.29}$$

$$V_{Ref} = V_n - n_q Q + \Delta V \tag{III.30}$$

Where $\Delta\omega$ and ΔV are the output signal of PI controllers that cancels the error between the nominal and the instantaneous frequency as well as the nominal and instantaneous voltage amplitude. Since the droop control is allowing an equal power sharing between the two inverters, the instantaneous voltage amplitude and frequency can be obtained from only one single inverter, then the two factors $\Delta\omega$ and ΔV can be divided between both inverters [24], this can be seen

in figure III.22 :

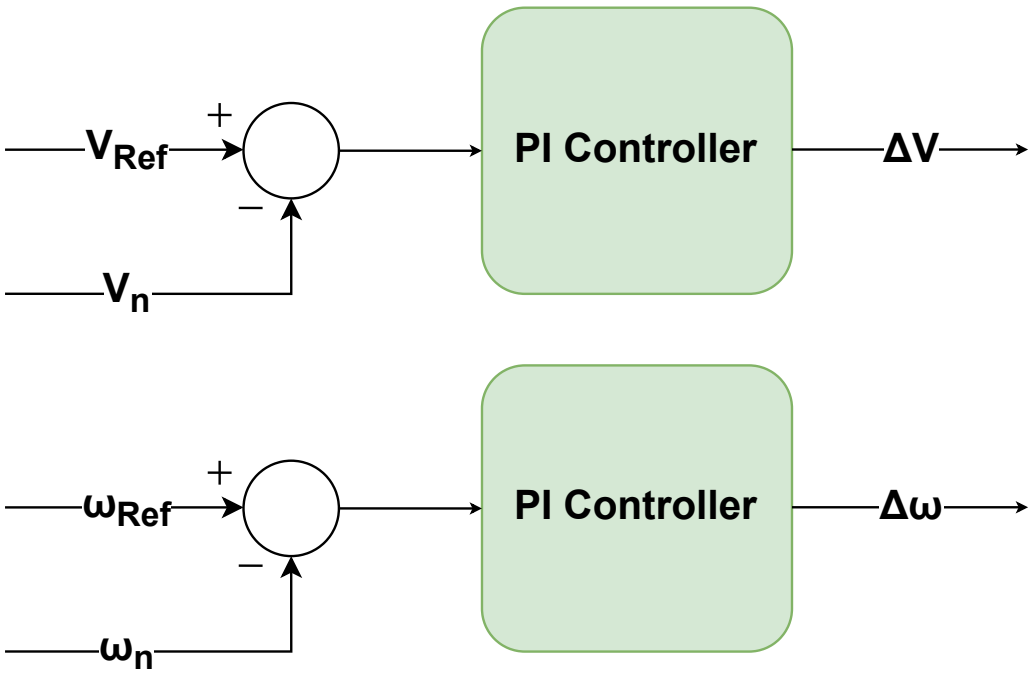

Figure III.22: Frequency and voltage amplitude restoration scheme

By doing a restoration to the voltage amplitude and the frequency, issues like the one we have met in the previous section are dealt with, for the simulation, the same exact voltage, load and power rating used in the droop section are used here, since this plant is unconditionally stable (Phase margin of 90 degrees and an infinite gain margin), the parameters of the two PI controllers are calculated to obtain a quick response and settling time. (0.231s and 0.406s respectively), they are set to $K_p = 0.05; K_i = 10$, the results are :

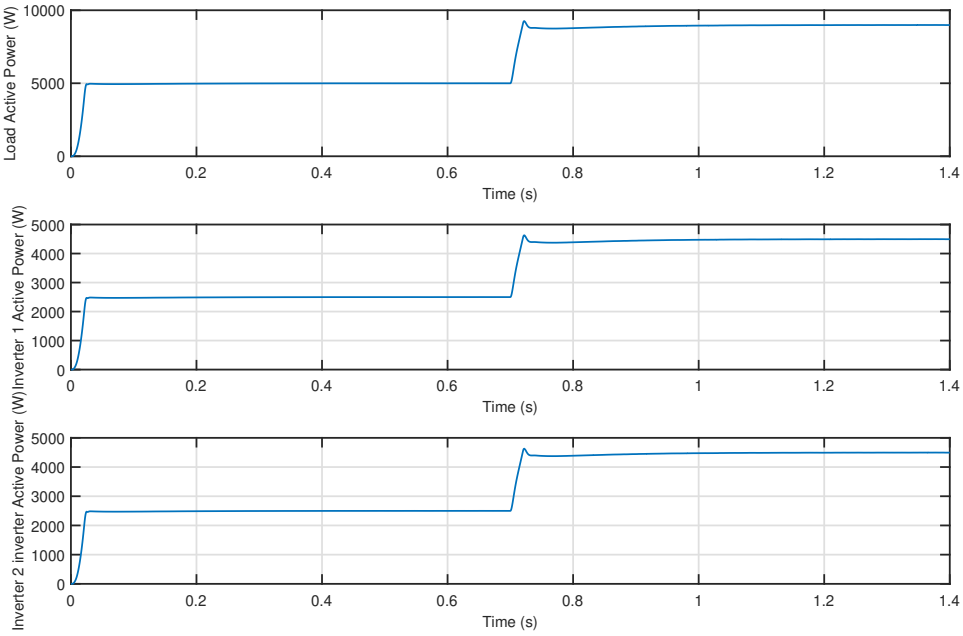

Figure III.23: Active power of the load and both inverters

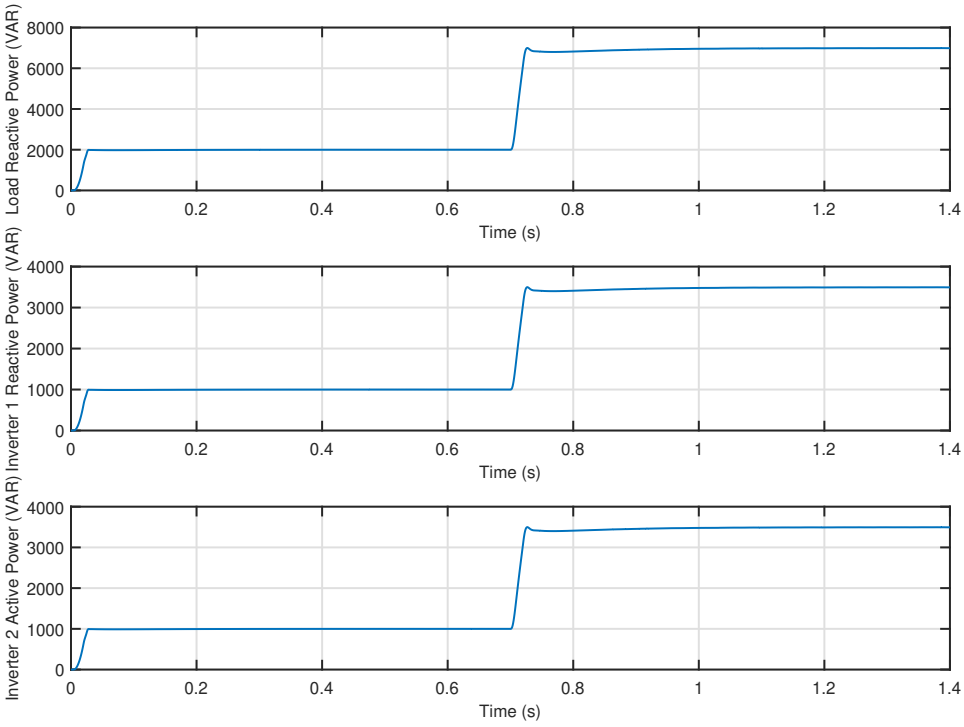

Figure III.24: Reactive power of the load and both inverters

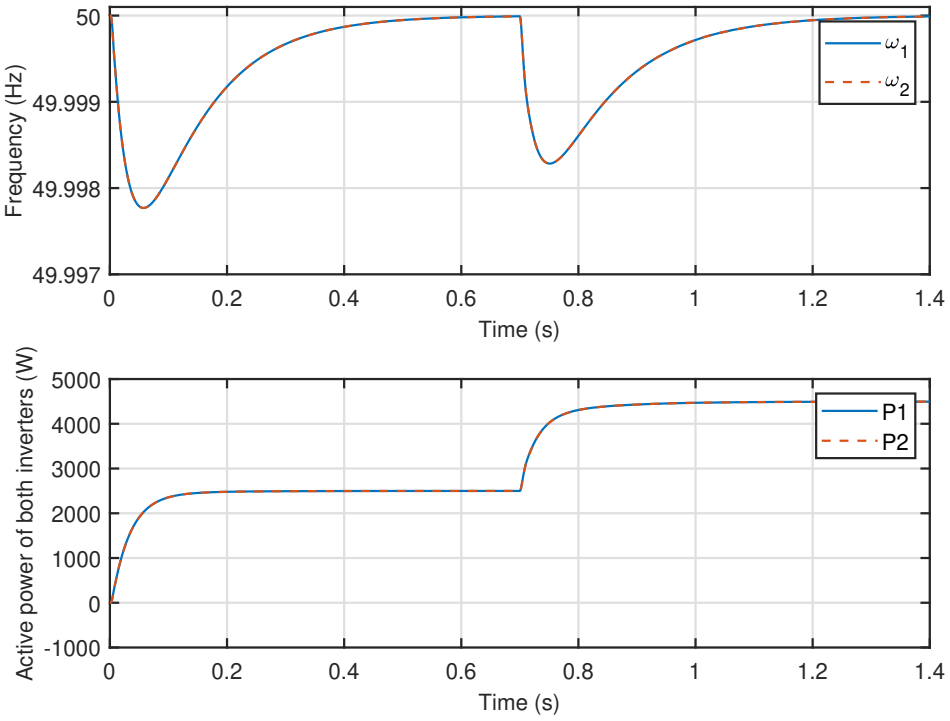

Figure III.25: Frequency and Active power of the two inverters

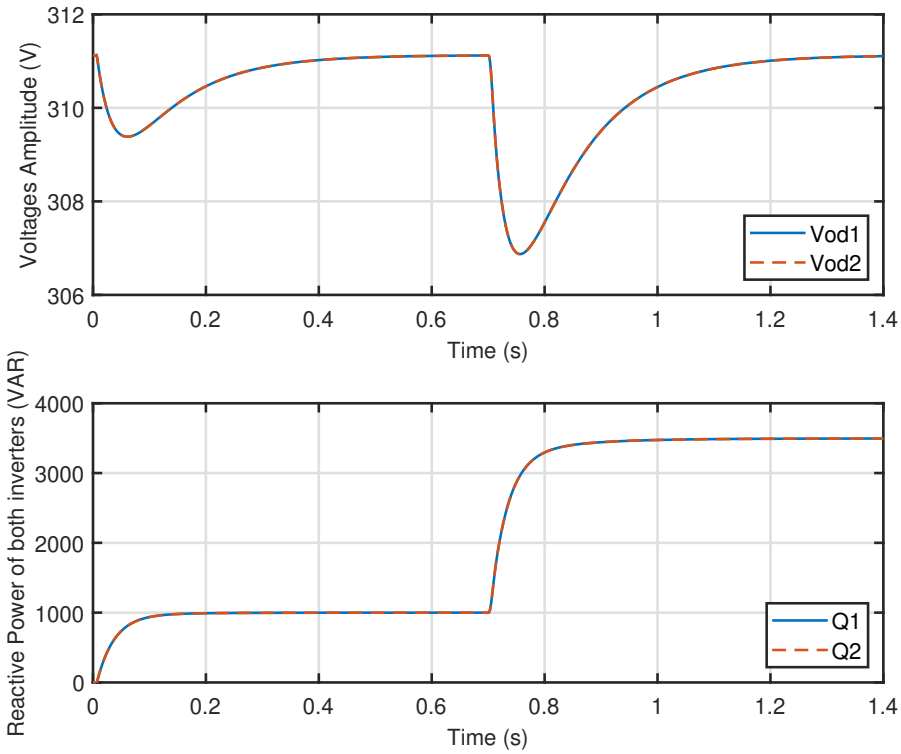

Figure III.26: Voltage amplitude and Reactive power of the two inverters

As we can see in the previous figures, especially in figures III.25 and III.26, the power demands applied by the load are exactly met and that is due to the accurate restoration of both the frequency and voltage's amplitude.

III.5 Conclusion

In this chapter, we have talked about the forming and following inverters as well as the sliding mode control method (the twisting algorithm specifically) applied to both of them.

After that, a centralized primary control method (Master/Slave control) is the subject of discussion, we have talked about how can this method perform power sharing between the forming and the following inverter, as well as some disadvantages regarding its reliability.

Finally, the decentralized primary control method (Droop control) is brought up to attention, we have talked about the workings of this method as well as its disadvantages when paired to loads with specific voltage and frequency ratings, to overcome these, the second level of microgrids control (Voltage amplitude and frequency restoration) is applied.

General Conclusion

In this dissertation, we had been interested in the implementation of microgrids and more specifically the control of parallel inverters that represent the most salient part of them. The main objective is to ensure the stability of the grid by balancing the power transfer between the sources and the utilization.

In the first chapter we provided some important notions of microgrids starting by their definition, their types, advantages and disadvantages, inverters and their types as well as the different control methods applied to microgrids.

The second chapter is where we talked about, first of all, the model of the inverter used in which we have proved its validity in details, then we have moved on to the presentation of the control methods used in this work, starting by the PID Controller in which we gave a brief definition of this method as well as some of the methods used to tune a PID Controller. Then we have concluded this chapter by the sliding mode control in which we gave a brief historical background and presented its two main types : First Order Sliding Mode and Higher Order Sliding Mode, with the implementation of Second Order Sliding Mode Control twisting algorithm.

For the third and final chapter, we moved to the simulation part of this work, starting by the level-zero control (or voltage and current control) by designing a working implementation of the twisting algorithm to control either the output voltage or current of an inverter in which we had great results (a response time less than 10ms) and an excellent reference tracking, then we have moved on to the primary control in which we have tried two methods : the centralised method of Master/Slave control for which we have obtained some good results when it comes to power sharing, but we ran into some issues like the inaccuracy of the power sharing in higher load demand situations and the fact that for this method to be implemented practically, a high bandwidth communication channels is needed, in which cost can play a significant role, for these issues, we implemented the decentralized method of droop control, this method allows equal power sharing between inverters by dropping the voltage's frequency and amplitude to properly meet the active and reactive power demands respectfully, but as we have mentioned in the first chapter, this method require the use of secondary control (or voltage's amplitude and frequency restoration), we were able to successfully implement this secondary control and restore the voltage's amplitude and frequency to their nominal values

For future works on this subject, Three points of improvements can be mentioned

- The first point is about validating the obtained results experimentally.
- The second point concerns the calculation and the generation of reference signal for the Master/Slave method to reject all harmonics present on it.
- The third point is about connecting the parallel inverter to the main grid to show the efficiency of the control techniques used in this work.

Bibliography

[1] Y. Ojo, M. Benmiloud, and I. Lestas, "Frequency and voltage control schemes for three-phase grid-forming inverters," *IFAC-PapersOnLine*, vol. 53, no. 2, pp. 13471–13476, 2020.

[2] N.Khefifi, *Élaboration de stratégies de contrôle-commande basées sur la passivité pour le pilotage d'un micro-réseau de génération décentralisée de type AC en mode autonome*. PhD thesis, UNIVERSITÉ DE NANTES, 2021.

[3] Z.Ghorzi and A.Mimouni, "Inverter control strategies," Master's thesis, Higher School in Applied Sciences, Tlemcen, 2019.

[4] M.Prodanovic, *Power Quality and Control Aspects of Parallel Connected Inverters in Distributed Generation*. PhD thesis, University of London Imperial College, 2004.

[5] A. Firdaus and S. Mishra, "Mitigation of power and frequency instability to improve load sharing among distributed inverters in microgrid systems," *IEEE Systems Journal*, vol. 14, no. 1, pp. 1024–1033, 2019.

[6] W. Perruquetti and J.-P. Barbot, *Sliding Mode Control In Engineering*. CRC Press, 2002.

[7] T. Floquet, *Contributions à la commande par modes glissants d'ordre supérieur*. PhD thesis, Lille 1, 2000.

[8] A. M. of Energy and Mining, "Energies nouvelles, renouvelables et maitrise de l'energie." `https://www.energy.gov.dz/?rubrique=energies-nouvelles-renouvelables-et-maitrise-de-lrenergie`. Accessed: 06-06-2022.

[9] A.Bouzid, *Élaboration d'une Méthode de Contrôle pour Améliorer la Robustesse d'un Micro Réseau Électrique*. PhD thesis, Université du Québec à Trois-Rivières, 2017.

[10] U. department of energy's official website, "How microgrids work." `https://www.energy.gov/articles/how-microgrids-work`, 2014. Accessed: 07-03-2022.

[11] T. Vandoorn, J. De Kooning, B. Meersman, and L. Vandevelde, "Review of primary control strategies for islanded microgrids with power-electronic interfaces," *Renewable and Sustainable Energy Reviews*, vol. 19, pp. 613–628, 2013.

[12] D. S. Laval, "Types of microgrids transforming the industry." `https://sustainablesolutions.duke-energy.com/resources/three-types-of-microgrids/`, 2021. Accessed: 08-03-2022.

[13] M.Paolone, T.Gaunt, X.Guillaud, M.Liserre, S.Meliopoulos, A.Monti, T.V.Cutsem, V.Vittal, and C.Vournas, "Fundamentals of power systems modelling in the presence of converter-interfaced generation," *Electric Power Systems Research*, vol. 189, p. 106811, 2020.

[14] G.Séguier and F.Labrique, *Power electronic converters: DC-AC conversion*. Springer Science & Business Media, 2012.

[15] A. Bidram, V. Nasirian, A. Davoudi, and F. L. Lewis, *Cooperative synchronization in distributed microgrid control*. Springer, 2017.

[16] P. Rodríguez, J. Pou, J. Bergas, J. I. Candela, R. P. Burgos, and D. Boroyevich, "Decoupled double synchronous reference frame pll for power converters control," *IEEE Transactions on Power Electronics*, vol. 22, no. 2, pp. 584–592, 2007.

[17] D.Labbaci and M.R.Bechar, "Phase-locked loop design for grid-connected converters under unbalanced grid conditions," Master's thesis, University of Amar Telidji, Laghouat, 2021.

[18] S. Bacha, I. Munteanu, and A. I. Bratcu, *Power Electronic Converters Modeling and Control - with Case Studies*. Advanced Textbooks in Control and Signal Processing, Springer, Sept. 2013.

[19] D. Lequesne, *Régulation PID: analogique, numérique, floue*. Hermes Science Publications, 2006.

[20] Y. Granjon, *Automatique*. Dunod, 2015.

[21] J.-J. E. Slotine, "Sliding controller design for non-linear systems," *International Journal of control*, vol. 40, no. 2, pp. 421–434, 1984.

[22] H. Han, X. Hou, J. Yang, J. Wu, M. Su, and J. M. Guerrero, "Review of power sharing control strategies for islanding operation of ac microgrids," *IEEE Transactions on Smart Grid*, vol. 7, no. 1, pp. 200–215, 2015.

[23] A. Mortezaei, M. G. Simões, M. Savaghebi, J. M. Guerrero, and A. Al-Durra, "Cooperative control of multi-master–slave islanded microgrid with power quality enhancement based on conservative power theory," *IEEE transactions on smart grid*, vol. 9, no. 4, pp. 2964–2975, 2016.

[24] F. Guo, C. Wen, J. Mao, and Y.-D. Song, "Distributed secondary voltage and frequency restoration control of droop-controlled inverter-based microgrids," *IEEE Transactions on industrial Electronics*, vol. 62, no. 7, pp. 4355–4364, 2014.